Title: Influence of sampling and disturbance history on climatic sensitivity of temperature-limited conifers

Authors:

Miloš Rydval[a,b], email: rydval@gmail.com, tel. (00420)735872634

Daniel L. Druckenbrod[c]

Miroslav Svoboda[a]

Volodymyr Trotsiuk[a,d,e]

Pavel Janda[a]

Martin Mikoláš[a]

Vojtěch Čada[a]

Radek Bače[a]

Marius Teodosiu[f,g]

Rob Wilson[b]

a. Faculty of Forestry and Wood Sciences, Czech University of Life Sciences Prague, Kamýcká 129, Praha 6–Suchdol, Prague, 16521, Czech Republic

b. School of Earth and Environmental Sciences, University of St Andrews, UK

c. Department of Geological, Environmental, & Marine Sciences, Rider University, Lawrenceville, NJ, USA

d. Swiss Federal Research Institute for Forest, Snow and Landscape Research (WSL), Birmensdorf, Switzerland.

e. Institute of Agricultural Sciences, ETH Zurich, Switzerland

f. “Marin Drăcea“ National Research and Development Institute in Forestry, Romania Voluntari, Romania

g. Faculty of Forestry, Ştefan cel Mare University of Suceava, Romania

ABSTRACT: Accurately capturing medium-to-low frequency trends in tree-ring data is vital to assessing climatic response and developing robust reconstructions of past climate. Non-climatic disturbance can affect growth trends in tree-ring width (RW) series and bias climate information obtained from such records. It is important to develop suitable strategies to ensure the development of chronologies that minimize these medium-to-low frequency biases. By performing high density sampling (760 trees) over a ~40ha natural high elevation Norway spruce *(Picea abies)* stand in the Romanian Carpathians, this study assessed the suitability of several sampling strategies for developing chronologies with an optimal climate signal for dendroclimatic purposes. There was a roughly equal probability for chronologies (40 samples each) to express a reasonable (r=0.3-0.5) to non-existent climate signal. While showing a strong high-frequency response, older/larger trees expressed the weakest overall temperature signal. Although random sampling yielded the most consistent climate signal in all sub-chronologies, the outcome was still sub-optimal. Alternative strategies to optimise the climate signal, including very high replication and principal component analysis, were also unable to minimize this disturbance bias and produce chronologies adequately representing climatic trends, indicating that larger scale disturbances can produce synchronous pervasive disturbance trends that affect a large part of a sampled population. The Curve Intervention Detection (CID) method, used to identify and reduce the influence of disturbance trends in the RW chronologies, considerably improved climate signal representation (from r=0.28 before correction to r=0.41 after correction for the full 760 sample chronology over 1909-2009) and represents a potentially important new approach for assessing disturbance impacts on RW chronologies. Blue intensity (BI) also shows promise as a climatically more sensitive variable which, unlike RW, does not appear significantly affected by disturbance. We recommend that studies utilizing RW chronologies to investigate medium to long-term climatic trends also assess disturbance impact on those series.

KEYWORDS: disturbance detection; sampling bias; climatic signal; blue intensity; tree rings; Norway spruce; Romanian Carpathian Mountains

INTRODUCTION

The accurate representation of climatic variability in the growth trends contained in tree-ring records from climatically sensitive trees is central to assessing growth-climate response and the development of robust dendroclimatic reconstructions (e.g. Anchukaitis et al., 2017; Cook et al., 2015; Cook et al., 2016; D'Arrigo et al., 2006; Luterbacher et al., 2016; Wilson et al., 2016). The suitability of strategically sampled tree-ring chronologies for reconstructing a particular climatic variable is typically evaluated by examining the growth-climate response and the strength of this relationship. This process partly relies on the assumption that chronologies are developed from a finite number of samples that are representative of the population. In climatically sensitive stands (i.e. temperature sensitive trees at high latitude or elevation tree-line locations) it is usually assumed that when adequate measures are taken to avoid sampling trees likely affected by non-climatic influences, the common signal of the sample chronology represents the common climatic signal of the population (Hughes, 2011).

Tree growth is the product of a range of environmental influences that are integrated into the annual growth increment (Cook, 1985; Vaganov et al., 2006). Natural disturbance is one key element of forest ecosystem development (Attiwill, 1994). The presence of non-climatic disturbance trends in tree ring width (RW) series complicates the development of climatically sensitive tree-ring based records (e.g. Briffa et al., 1996; Gunnarson et al., 2012; Rydval et al., 2016). Yet few, if any, studies explicitly assess the influence of disturbance as a part of dendroclimatic research. A common presumption is that the effects of disturbance are either negligible or asynchronous so that their influence is canceled out through the development of a mean chronology of detrended series, or they can be minimized by applying appropriate detrending techniques in cases when such trends occur systematically (Hughes, 2011). It has been shown that larger scale intermediate and higher severity disturbances can result in synchrony of disturbance histories across the landscape on the stand level and regional spatial scales (e.g. D'Amato and Orwig, 2008; Kulakowski and Veblen, 2002; Zielonka et al., 2010). While flexible data-adaptive detrending approaches such as cubic smoothing splines (Cook and Peters, 1981) have been utilized to limit the influence of non-climatic (e.g. disturbance) trends in RW data, a detrimental side-effect of such techniques is the loss of lower frequency (i.e. multidecadal to multicentennial) climatic variability.

Numerous studies have investigated dendrochronological biases and uncertainties related to various methodological aspects of tree-ring data development including detrending (e.g. Briffa and Melvin, 2011;Cook et al., 1995; Helama et al., 2004; Melvin and Briffa, 2008; Melvin et al., 2013)*,* sample size and signal strength (e.g. Mérian et al., 2013; Osborn et al., 1997; Wigley et al., 1984), sampling design and microsite conditions (e.g. Cherubini et al., 1998; Düthorn et al., 2013, 2015; Nehrbass-Ahles et al., 2014), and tree age (e.g. Carrer and Urbinati, 2004; Esper et al., 2008; Fish et al., 2010). In an extensive assessment of sampling design strategies, Nehrbass-Ahles et al. (2014) highlighted that many common sampling approaches used for developing representations of forest response to environmental change can induce sampling related biases. However, relatively little is known about how disturbance related growth trends affect the climate signal in tree ring series.

Time-series analysis with intervention detection (Box and Jenkins, 1970; Box and Tiao, 1975) is an evolving area for studying disturbance in RW data (Druckenbrod, 2005). A time-series based method called Curve Intervention Detection (CID) has been developed to characterize disturbance history and quantify the effects of disturbance trends on individual RW series and overall chronology structure (Druckenbrod, 2005; Druckenbrod et al., 2013). Chronology distortion and climate signal degradation, due to synchronous disturbance related growth releases as a result of systematic timber felling, was identified using the CID technique by Rydval et al. (2016) in Scots pine RW chronologies from Scotland. However, such a technique has not previously been applied to investigate trends resulting from natural sources of disturbance on the strength of the climate signal in tree-ring records.

Building on the work of Rydval et al. (2016), in this study we applied the CID method to a new forest system and species by examining RW series from an unmanaged natural closed canopy Norway spruce (*Picea abies*) stand in Romania (shaped by a mixed-severity natural disturbance regime with partial landscape synchronization and unperturbed by human activities - Svoboda et al., 2014) to examine the extent to which natural disturbance can affect climate signal strength in RW data. We investigate (1) whether natural disturbance can produce widespread and synchronized trends, as those resulting from human activities, that would significantly impact the expression of the climate signal in tree-ring chronologies, and (2) which sampling or data processing approach best expresses the climate signal. To this end, we firstly evaluated a set of sampling strategies by subsampling a large dataset of RW data from a single stand according to a set of characteristics reflecting sampling strategies that are relevant in a dendroclimatic context. The application of additional data processing techniques (including disturbance trend detection and correction using the CID method, and isolation of the dominant signals through principal component analysis) were investigated in an attempt to optimize the climate signal. We applied the CID time-series analysis technique in order to characterize the disturbance history, its impact on overall chronology structure and subsequently to reduce the influence of disturbance-related trends on RW chronologies (Druckenbrod, 2005; Druckenbrod et al., 2013; Rydval et al.,2016). As an alternative to RW data, a subset of chronologies was developed from series of the blue intensity (BI) parameter (Björklund et al., 2014a; McCarroll et al., 2002; Rydval et al., 2014) to ascertain whether such data can be used to produce proxy climate records unbiased (or less biased) by the presence of disturbance trends.

METHODS

Sampling site

Samples were collected and measured from 760 high-elevation Norway spruce (*Picea abies*) trees (cored at breast height) located in an approx. 40 ha natural Norway spruce dominant stand (47°06’53”N,25°15’26”E) in Călimani National Park (hereafter Calimani) in the Eastern Carpathians of northern Romania (Figure 1; see Svoboda et al. (2014) for details regarding sample collection). The selected sampling site is located within an elevational range of around 1500-1650 m a.s.l., ~100-250 m below the regional timberline (approx. 1780 m a.s.l.) and ~200-350 m below the treeline (approx. 1860 m a.s.l.) (Popa and Kern, 2009) and with slope varying from around 10° to 25°. Podzols are the predominant soil type in the study region (Valtera et al., 2013). The area has a mean annual temperature of 2.1-3.1°C estimated from 0.5° gridded CRU TS3.23 temperatures (based on the period 2005-2014 and adjusted for elevation). Over the same period, temperatures have increased by approximately 1.6°C relative to the first decade of the 20th century. Mean annual precipitation is about 910 mm (2005-2014 mean).

[insert Figure 1]

Sample collection was performed in an area with no significant human activities in the past (including evidence from historical documentation) and subject only to natural stand dynamics and disturbance regimes (Svoboda et al., 2014). Considering the size of the sampled area and number of samples collected, this high density sampling strategy, similar to that of Nehrbass-Ahles (2014), was intended to provide a highly representative sample of the whole stand population by sampling a diverse range of tree size and age classes. This approach makes it possible to group samples and construct chronologies according to a range of characteristics.

CHRON. (SUBSET)	NR. OF SERIES	MEAN ELEVATION	CHRON. LENGTH	EPS ≥ 0.85	CHRON. (BY DBH)	DBH RANGE (CM)	CHRON. (BY AGE)	AGE RANGE
PLOT-ALL	760	1578	1673-2009	1744-2009		110-925		31-337
PLOT-1	40	1523	1731-2009	1888-2009	DBH-1	110-235	AGE-1	31-82
PLOT-2	40	1585	1724-2009	1862-2009	DBH-2	235-265	AGE-2	82-85
PLOT-3	40	1602	1743-2009	1906-2009	DBH-3	265-280	AGE-3	85-87
PLOT-4	40	1616	1772-2009	1905-2009	DBH-4	280-300	AGE-4	87-89
PLOT-5	40	1588	1768-2009	1820-2009	DBH-5	300-320	AGE-5	89-92
PLOT-6	40	1626	1790-2009	1857-2009	DBH-6	320-340	AGE-6	92-97
PLOT-7	40	1633	1712-2009	1835-2009	DBH-7	340-360	AGE-7	97-111
PLOT-8	40	1516	1673-2009	1897-2009	DBH-8	360-380	AGE-8	112-118
PLOT-9	40	1514	1700-2009	1903-2009	DBH-9	380-400	AGE-9	118-122
PLOT-10	40	1606	1763-2009	1835-2009	DBH-10	400-415	AGE-10	122-127
PLOT-11	40	1565	1701-2009	1856-2009	DBH-11	415-430	AGE-11	127-134
PLOT-12	40	1587	1763-2009	1906-2009	DBH-12	430-450	AGE-12	134-142
PLOT-13	40	1590	1768-2009	1896-2009	DBH-13	450-480	AGE-13	142-148
PLOT-14	40	1552	1705-2009	1861-2009	DBH-14	480-500	AGE-14	148-156
PLOT-15	40	1551	1720-2009	1901-2009	DBH-15	500-520	AGE-15	156-162
PLOT-16	40	1541	1803-2009	1909-2009	DBH-16	520-550	AGE-16	163-176
PLOT-17	40	1511	1752-2009	1903-2009	DBH-17	550-590	AGE-17	176-201
PLOT-18	40	1552	1757-2009	1902-2009	DBH-18	590-650	AGE-18	201-234
PLOT-19	40	1572	1750-2009	1838-2009	DBH-19	651-925	AGE-19	235-337

Table 1: Site and chronology descriptive information. PLOT represents chronologies developed according to sample location (i.e. plot-based), DBH chronologies are composed of samples grouped according to diameter at breast height, and AGE represents chronologies with samples grouped according to tree recruitment age. With the exception of the PLOT-ALL chronology, all other chronologies were developed using 40 samples. (EPS = expressed population signal, Wigley et al., 1984).

Data analysis

Sampled cores were mounted and glued on wooden mounts and subsequently surfaced with a blade to enhance the visibility of ring boundaries. To help determine tree recruitment age (i.e. the number of rings at coring height), pith-offset was estimated using an acetate sheet with concentric circles. However, the method of sample collection specifically focused on minimizing pith-offset and so the majority of samples included the pith. Ring width was then measured using a LINTAB traversing measuring stage coupled with TsapWin (RINNTECH, Germany) measuring software to a precision of 0.01 mm. Sample crossdating was performed using standard dendrochronological approaches (Stokes and Smiley, 1968) and crossdating of measured series was checked with CDendro (Larsson, 2015).

Disturbance detection and correction

Curve Intervention Detection (CID) is a time-series intervention detection method based on the work of Druckenbrod (2005) and Druckenbrod et al. (2013). The method was used here to objectively identify and remove disturbance trends from individual RW series following the procedure described in Rydval et al. (2016), where it was used to identify and correct for growth release trends due to logging-related disturbance in Scottish Scots pine (*Pinus sylvestris*) samples. In this study, both growth release and growth suppression trends were detected and removed. Prior to the CID procedure, a constant of 1 mm was added to all measurements to avoid the possibility of losing tree-ring information during the disturbance removal procedure (Rydval et al., 2016). As part of the CID procedure, RW measurement series were first power transformed (Cook and Peters, 1997) and then detrended by fitting a negative exponential or linear function. Disturbance trends were identified as outliers from 9-30 year running mean distributions based on the residual series of each detrended RW series and autoregressive model estimates. The identified release / suppression trend was removed by subtracting a curve (Warren, 1980) fitted to the series from the point where the initiation of the disturbance-related trend was identified. The procedure was repeated until no further outliers were detected. The disturbance-corrected series were then re-expressed in the original (non-detrended) measurement format so that both the corrected and uncorrected series could then be detrended in the same way. For a detailed description of the method refer to Rydval et al. (2016). CID (ver. 1.05) was used in these analyses and is included in the supplemental materials as Matlab code files. A freely-available executable (ver. 1.07) is available using the Matlab compiler. Contact Daniel Druckenbrod (ddruckenbrod@rider.edu) as this version is dependent on operating system and Matlab release version. These time-series methods are a work in progress, but we also welcome other researchers to experiment with this tool to detect and isotlate disturbance events in ring-width series.

RW chronology development

Two sets of chronologies were developed with the first set composed of series prior to disturbance correction using the CID method (i.e. uncorrected for the influence of disturbance – pre-CID) and the second set using series after correcting for disturbance trends with CID (post-CID). Using ARSTAN (Cook and Krusic, 2005), both sets of RW series were power transformed to stabilize series variance (Cook and Peters, 1997) and detrended by subtracting negative exponential or negatively sloping linear functions. The mean chronology index was calculated using Tukey's robust bi-weight mean to reduce the influence of outlier values (Cook and Kairiukstis, 1990). Variance stabilization of the mean chronology, due to changing replication, was then performed according to the procedure described in Osborn et al. (1997).

In addition to developing an uncorrected (pre-CID) and disturbance corrected (post-CID) mean chronology from all 760 samples, the entire collection of series was also divided into 19 separate sub-plot chronologies (each including 40 series) compiled by grouping series according to 1) the plot location where the samples were collected (PLOT) (Figure 1); 2) random sample selection without replacement (RAN); 3) tree recruitment age (AGE), 4) and the diameter at breast height (DBH) (Table 1). All chronologies were truncated based on an expressed population signal (EPS – Wigley et al., 1984) cut-off of EPS ≥ 0.85.

Principal Component (PC) analysis, with varimax rotation, was applied using the IBM SPSS (v.20.0) statistical package (SPSS, 2011) to both pre-CID and post-CID location-based (PLOT) chronologies to reduce the dimensionality of the RW predictor dataset in order to extract the dominant modes of variance. Based on the temporal span of the shortest chronology (Table 1), the period 1909-2009 was used in order to include all chronologies in the analysis. Only the lowest order PC scores with an eigenvalue >1 were retained.

Blue Intensity chronology development

Similar to maximum latewood density, blue intensity (BI) represents summer growing conditions usually reflecting a (late) summer response to temperature in conifers from temperature limited locations (e.g. Björklund et al., 2014b; McCarroll et al., 2013; Rydval et al., 2014; Wilson et al., 2014). BI measurements were developed for a subset of the samples (three chronologies – PLOT-3, PLOT-7 and PLOT-10; 40 samples each) following Rydval et al. (2014). Since, unlike other conifers such as pine, Norway spruce samples do not exhibit any apparent visual colour difference between the heartwood and sapwood that would affect BI measurements, chemical treatment involving sample resin extraction was not performed. Such an approach was also considered adequate in a study by Wilson et al. (2014) examining BI data from Engelmann spruce in British Columbia. Samples surfaced with sanding paper up to 1200 grit grade were scanned using an Epson Expression 10000 XL flatbed scanner combined with SilverFast Ai (v.6.6 - Laser Soft Imaging AG, Kiel, Germany) scanning software. Scanner calibration was performed with the SilverFast IT8 calibration procedure using a Fujicolor Crystal Archive IT8.7/2 calibration target. A resolution of 2400 dpi was used for scanning. During the scanning process, samples were covered with a black cloth to prevent biases due to ambient light.

CooRecorder measurement software (Larsson, 2015) was used to measure BI from scanned images. The BI series were then inverted according to Rydval et al. (2014) to express a positive relationship with RW and instrumental temperatures and subsequently detrended by subtraction from fitted negatively sloping linear functions. The mean BI chronology was calculated and truncated (EPS = 0.85) in the same way as the RW chronologies.

Climate data

For this study, in order to allow the assessment of the longest possible temporal span of the tree-ring data, we used mean temperature series from a meteorological station in Sibiu, Romania (hereafter SIBIU) covering the period 1851-2015 (data for 1918 were unavailable and were estimated from the relevant 0.5° CRU TS3.23 grid scaled to SIBIU) located approximately 170 km to the SSW of

Calimani (Figure 1). An additional temperature record was composited using the longest Central and Eastern European instrumental records in order to assess the whole span of the full 760 sample Calimani chronology. This Central/East European (CEU) composite covers the period 1773-2014 and includes temperature series from Prague (Czech Republic), Vienna (Austria), Kraków (Poland), Budapest (Hungary), Lviv (Ukraine) and Kishinev (Moldova). The individual instrumental series were converted to anomalies relative to 1961-1989 and combined as a simple average. To adjust for variance changes due to the changing number of series in the composite through time, the variance of the mean series was adjusted according to Osborn et al. (1997). Climate data were used to assess the strength of the climatic signal in tree ring chronologies using the Pearsons correlation coefficient (r).

RESULTS

Four sets of chronologies developed according to various sampling strategies are presented in Figure 2 with additional chronology information in Table 1. As the strongest significant chronology response was observed with June-July mean temperatures (see supplementary Figure S1), RW chronologies were assessed using this seasonal window. This seasonal response agrees with Sidor et al. (2015) who also noted a significant June-July mean temperature signal in high-elevation spruce sites in the Romanian Carpathians including Calimani.

The location-based 'PLOT' chronologies (Figure 2a – see Figure 1 for plot locations) displayed a large range of variability (especially before ~1960) which is also reflected in the wide range of variation in correlation between each chronology and June-July average instrumental temperatures (r = 0.07 to 0.46; $r_{\bar{x}}$ = 0.26 – Table 2). The 'RAN' chronologies based on random selection of samples (without replacement; Figure 2b) produced a more uniform range of variability which was also observed in the relationship between the chronologies and instrumental temperatures (r = 0.24 to 0.35; $r_{\bar{x}}$ = 0.26 – Table 2). When compared with the PLOT chronologies, the correlation range of these 'random sample' chronologies against instrumental temperatures was considerably narrower, although the mean correlation was virtually the same and while the very low correlations were no longer observed, the higher correlations were also no longer present. When grouped according to stem size (i.e. DBH – Figure

2c), chronologies displayed considerable variability particularly in the first half of the 20th century as well as in the most recent period (i.e. after ~1990). Chronologies composed of series from broader-stemmed (higher DBH) trees tended to correlate more weakly with instrumental temperatures (r = - 0.06 to 0.28 for chronologies DBH-12 – DBH-19; see Table 3 for details), whereas trees with narrower stems (lower DBH) appeared to exhibit higher correlations (r = 0.37 to 0.47 for chronologies DBH-1 – DBH-11 excluding the weaker DBH-9 chronology; see Table 3). The chronologies grouped according to age showed a similar range of variability to the DBH-based chronologies (Figure 2d). Although not as clear, there was a tendency for younger chronologies to correlate more strongly than the oldest chronologies (Figure 2d; Table 3). However, when examining only the high frequency (inter-annual) relationship between the chronologies and temperature (1st differenced results in Table 3), there was little difference between the young and old tree chronologies and larger trees actually displayed a stronger signal than chronologies from smaller trees (r = 0.30 to 0.43, $r_{\bar{x}}$ = 0.38 for chronologies DBH-1 – DBH-11; r = 0.42 to 0.51, $r_{\bar{x}}$ = 0.47 for chronologies DBH-12 – DBH-19). Unsurprisingly, a strong relationship (r = 0.63) was observed between age and DBH (Figure S2), which indicates that older trees generally also tend to be larger (i.e. higher DBH) and vice-versa.

[insert Figure 2]

SAMPLING TYPE	PRE-CID	POST-CID	1ST DIFFERENCED
LOCATION (PLOT) (1909-2009)	$r_{\bar{x}}$ = 0.255 ± 0.124 r_{range}= 0.066 - 0.461	$r_{\bar{x}}$ = 0.383 ± 0.126 r_{range} = 0.079 - 0.540	$r_{\bar{x}}$ = 0.422 ± 0.044 r_{range} = 0.337 – 0.530
RANDOM (1912-2009)	$r_{\bar{x}}$ = 0.265 ± 0.057 r_{range} = 0.183 - 0.381	$r_{\bar{x}}$ = 0.401± 0.049 r_{range} = 0.329 - 0.505	$r_{\bar{x}}$ = 0.441 ± 0.032 r_{range} = 0.387 – 0.503
DBH (1917-2009)	$r_{\bar{x}}$ = 0.265 ± 0.174 r_{range}= -0.067 - 0.472	$r_{\bar{x}}$ = 0.379 ± 0.062 r_{range}= 0.263 - 0.489	$r_{\bar{x}}$ = 0.414 ± 0.059 r_{range}= 0.297 – 0.508
AGE (1933-2009)	$r_{\bar{x}}$ = 0.309 ± 0.153 r_{range} = -0.067 - 0.483	$r_{\bar{x}}$ = 0.397 ± 0.081 r_{range} = 0.236 - 0.509	$r_{\bar{x}}$ = 0.377 ± 0.066 r_{range} = 0.255 – 0.485

Table 2: Average correlation and correlation range of chronologies before (pre-CID) and after (post-CID) disturbance correction and first differenced chronologies developed with different sampling strategies, including samples grouped by location (PLOT), random sample selection (RAN), grouping according to diameter at breast height (DBH), and sample age (AGE), against SIBIU Jun-Jul mean instrumental temperatures. ($r_{\bar{x}}$ represents the mean correlation ± 1 standard deviation, while r_{range} represents the full correlation range)

CHRON. (RANDOM)	PRE-CID CORR	POST-CID CORR	1ST DIFF CORR	CHRON. (BY DBH)	PRE-CID CORR	POST-CID CORR	1ST DIFF CORR	CHRON. (BY AGE)	PRE-CID CORR	POST-CID CORR	1ST DIFF CORR
RAN-1	0.318	0.505	0.471	**DBH-1**	0.473	0.453	0.297	**AGE-1**	0.374	0.339	0.294
RAN-2	0.239	0.436	0.503	**DBH-2**	0.373	0.311	0.331	**AGE-2**	0.483	0.451	0.421
RAN-3	0.279	0.473	0.471	**DBH-3**	0.393	0.418	0.351	**AGE-3**	0.414	0.440	0.353
RAN-4	0.218	0.406	0.480	**DBH-4**	0.402	0.396	0.369	**AGE-4**	0.473	0.452	0.431
RAN-5	0.246	0.380	0.475	**DBH-5**	0.402	0.389	0.389	**AGE-5**	0.446	0.509	0.449
RAN-6	0.248	0.381	0.415	**DBH-6**	0.397	0.358	0.390	**AGE-6**	0.470	0.489	0.414
RAN-7	0.300	0.329	0.451	**DBH-7**	0.406	0.368	0.344	**AGE-7**	0.362	0.433	0.309
RAN-8	0.381	0.406	0.417	**DBH-8**	0.471	0.489	0.426	**AGE-8**	0.370	0.323	0.321
RAN-9	0.241	0.407	0.471	**DBH-9**	0.196	0.327	0.387	**AGE-9**	0.348	0.267	0.338
RAN-10	0.228	0.405	0.397	**DBH-10**	0.403	0.390	0.433	**AGE-10**	0.237	0.310	0.352
RAN-11	0.301	0.379	0.441	**DBH-11**	0.357	0.409	0.429	**AGE-11**	0.258	0.309	0.307
RAN-12	0.334	0.434	0.439	**DBH-12**	0.135	0.353	0.418	**AGE-12**	0.227	0.334	0.255
RAN-13	0.183	0.349	0.387	**DBH-13**	0.275	0.353	0.451	**AGE-13**	0.356	0.390	0.338
RAN-14	0.359	0.487	0.414	**DBH-14**	0.182	0.464	0.507	**AGE-14**	0.414	0.489	0.381
RAN-15	0.187	0.360	0.436	**DBH-15**	0.054	0.394	0.454	**AGE-15**	0.348	0.430	0.401
RAN-16	0.247	0.334	0.429	**DBH-16**	0.145	0.457	0.496	**AGE-16**	0.034	0.470	0.485
RAN-17	0.238	0.368	0.415	**DBH-17**	-0.067	0.302	0.433	**AGE-17**	0.217	0.443	0.386
RAN-18	0.300	0.402	0.456	**DBH-18**	0.110	0.300	0.453	**AGE-18**	0.109	0.435	0.469
RAN-19	0.197	0.370	0.411	**DBH-19**	-0.064	0.263	0.508	**AGE-19**	-0.067	0.236	0.467

Table 3: Correlations of chronologies before (pre-CID) and after (post-CID) disturbance correction and first differenced chronologies sampled using different sampling strategies, including random sample selection (RAN), grouping according to diameter at breast height (DBH), and sample age (AGE), against Jun-Jul mean instrumental temperatures from Sibiu (shading is used to aid interpretation of the results with darker shades indicating higher correlations).

A summary of the general disturbance history at Calimani is provided in Figure 3a. The results showed three major pulses or clusters of disturbance events, which affected a large proportion of the stand, detected in the 1740s, the middle of the 19th century and the 1910s followed by growth releases in the subsequent decades attributable to those disturbances. Disturbance suppression events were detected in the mid/late 18th century, although the predominant release events were more prevalent whereas suppression events did not appear to considerably affect the mean disturbance chronology. The pre- and post- correction chronologies (Figure 3b and 3c respectively) indicated a wider spread in individual pre-CID chronologies and greater deviation from the mean chronology compared to their post-CID counterparts. This was also observed with the other sampling approaches (Table 2). The disturbance growth chronology in Figure 3a identified periods of growth release pulses attributable to disturbance which are evident in the Figure 3b mean chronology. After disturbance correction, the spread of the individual chronologies was reduced as the growth release trends were removed and the post-CID chronologies exhibited greater similarity to the mean chronology which did not contain the growth release trends. The mean pre- and post-CID chronologies are displayed together with the SIBIU instrumental temperature record (back to 1851) and the Central European (CEU) instrumental temperature composite extending back to the 1770s (Figure 3d). The main differences between the corrected and uncorrected chronologies become apparent with lower post-correction RW index values in the first half of the 20th century and higher values from approximately 1770 until 1850. These results also highlighted the improved agreement of the post-CID chronology with both the shorter SIBIU ($r_{pre\text{-}CID}$ = 0.27; $r_{post\text{-}CID}$= 0.36) and longer CEU ($r_{pre\text{-}CID}$ = 0.14; $r_{post\text{-}CID}$= 0.26) instrumental temperature series.

[insert Figure 3]

The change in correlation between individual pre-CID and post-CID chronologies and the SIBIU temperature series for the common 1909-2009 period (Figure 4a) showed overall improvement of the mean chronology as well as all individual chronologies with the exception of PLOT-16. Similar results were obtained when evaluating the full length of each chronology (Figure 4c). A comparison of the pre- and post-CID root-mean-square error (RMSE) results for the common 1909-2009 period (Figure 4b) and the full length of overlap (Figure 4d) between individual PLOT chronologies and SIBIU indicated a RMSE decrease in nearly all post-CID chronologies. This RMSE pattern largely mirrored the correlation change results and indicated chronology improvement in the sense that lower RMSE results were observed in the post-correction chronologies. The results from Figure 4c were also represented spatially in Figure 1. The greatest degree of post-CID chronology correlation increase with instrumental temperatures was observed in chronologies from the southeastern slope, which predominantly contained growth release trends in the first half of the 20th century. Chronologies showing intermediate improvement were located farther north and included chronologies from the northwestern slope which predominantly contained disturbance related trends in the second half of the 19th century. The least improvement was observed in chronologies from the northwestern (PLOT-1) and northernmost (PLOT-18) investigated locations as well as on the southern ridge (PLOT-6) and in the valley (PLOT-16), with the latter two chronologies exhibiting no late 19th / early 20th century disturbance trends. Supplementary Figure S3 highlights in greater detail this broad spatial and temporal split in the pattern of disturbance of the northwest / southeast groups and the very large percentage of trees in each group affected by these two major disturbance events. Individual chronologies developed according to the other sampling strategies showed an overall pattern of post-CID improvement similar to the location based (PLOT) assessment (Table 3). The pre-CID and post-CID results from Table 3 along with their respective chronologies are displayed graphically in supplementary Figure S4.

[insert Figure 4]

The principal component (PC) time-series scores of the dominant modes of variance of the pre-CID dataset are presented in Figure 5a and include three PCs (loadings of the chronologies on each eigenvector are presented in Table 4). PC3 showed the strongest correlation with SIBIU Jun-Jul temperatures (r = 0.45) and PC1 correlated more weakly (r = 0.33), while PC2 was weakly negatively correlated with temperatures (r = -0.24). When compared to the disturbance chronology in Figure 3a, a strong correlation was observed with PC2 (r = 0.91). After CID correction, only two dominant PCs were identified. Although the first PC was uncorrelated with temperatures, a stronger relationship was observed between temperature and PC2 (r = 0.56) than was identified with any of the pre-CID PC scores. Conversely, PC1 significantly correlated with the disturbance chronology (r = 0.50), whereas no correlation was found with PC2.

[insert Figure 5]

CHRON. (SUBSET)	PC1 (PRE-CID)	PC2 (PRE-CID)	PC3 (PRE-CID)	CHRON. (SUBSET)	PC1 (POST-CID)	PC2 (POST-CID)
PLOT-10	**0.911**	0.163	0.275	PLOT-1	**0.932**	0.157
PLOT-5	**0.907**	0.216	0.168	PLOT-11	**0.878**	0.358
PLOT-19	**0.885**	0.302	0.265	PLOT-14	**0.875**	0.244
PLOT-2	**0.826**	0.350	0.301	PLOT-19	**0.827**	0.472
PLOT-1	**0.813**	0.528	-0.071	PLOT-6	**0.791**	0.508
PLOT-9	**0.741**	0.436	0.403	PLOT-10	**0.791**	0.478
PLOT-11	**0.703**	0.625	0.160	PLOT-2	**0.777**	0.530
PLOT-7	**0.603**	0.460	0.576	PLOT-8	**0.772**	0.374
PLOT-8	0.414	**0.828**	0.312	PLOT-5	**0.721**	0.402
PLOT-14	0.535	**0.795**	0.156	PLOT-7	**0.718**	0.601
PLOT-15	0.356	**0.761**	0.461	PLOT-9	**0.714**	0.585
PLOT-3	0.377	**0.758**	0.448	PLOT-16	0.112	**0.876**
PLOT-4	0.377	**0.692**	0.536	PLOT-4	0.337	**0.858**
PLOT-6	0.551	**0.652**	0.481	PLOT-13	0.367	**0.858**
PLOT-16	0.121	0.010	**0.934**	PLOT-17	0.438	**0.815**
PLOT-12	0.173	0.518	**0.803**	PLOT-12	0.539	**0.788**
PLOT-18	0.413	0.337	**0.776**	PLOT-15	0.523	**0.780**
PLOT-13	0.138	0.579	**0.723**	PLOT-3	0.529	**0.772**
PLOT-17	0.270	0.582	**0.710**	PLOT-18	0.587	**0.635**

Table 4: Principal Component (PC) Analysis loadings of location-based (PLOT) chronologies before (pre-CID) and after (post-CID) disturbance correction on the dominant eigenvectors (results in bold indicate the strongest loading of each chronology).

The restricted three site (PLOT3, 7 and 10) correlation response analysis assessing the relationship between pre-CID, post-CID and BI data, with SIBIU temperatures (- Figure 6a) clearly shows disturbance trends in the RW data with various degrees of post-CID improvement. In contrast to the relatively narrow RW seasonal response, the BI chronology responded more strongly to a broader seasonal window displaying highest correlations with mean July-September temperatures (r = 0.65). The response of BI was stronger than post-CID RW with respect to the optimal season of each parameter. Although improvement of the post-CID chronologies (Figures 6b, c and d) was apparent especially before 1880 when the deviation of the pre-CID chronology from the instrumental record was reduced, the degree of improvement was limited, particularly as periods of weaker agreement remained as indicated by running correlations between the pre-/post-CID chronologies and SIBIU temperatures. In contrast, the BI chronologies more closely matched the instrumental trends with running correlations displaying a consistently strong relationship back into the 19th century.

[insert Figure 6]

DISCUSSION

Considering the relatively small area of the Calimani study area, it would be reasonable to assume that chronologies developed from the plots would be similar in the absence of disturbance and should therefore also express a very similar climate signal. However, despite the adequate replication of the different chronologies, a range of chronology trends were observed (Figure 2a) expressing substantial differences in correlation with temperature ranging from zero to ~0.5. The possibility of developing a climatically sensitive chronology by randomly choosing and sampling all trees in a specific plot would therefore depend on chance. An alternative approach, which randomly samples trees from the whole stand (Figure 2b), produced a more consistent and uniform outcome, although generally resulting in correlations of only ~0.3 with temperature.

A sampling strategy commonly applied for dendroclimatology favours the preferential selection of larger / wider (i.e. higher DBH) and presumed older trees in order to extend a chronology as far back in time as possible. The strong age / DBH relationship (Figure S2), would support this type of reasoning.

Forming chronologies by grouping series according to DBH, revealed that samples from the largest trees expressed the weakest temperature signal (Figure 2c). Although less clear-cut than the DBH results, there was also a tendency for chronologies composed of samples from old trees to produce a climatically weaker signal. Yet the 1stdifferenced results indicate that there is no fundamental limitation in the ability of older trees to record climatic information and that, at least at high frequencies, the sensitivity of larger trees compared to smaller ones is actually greater. This observation demonstrates that the overall response of trees does not simply weaken with age but is instead related to the presence of disturbance related trends that bias the lower frequency expressed in the data after detrending.

It would therefore be reasonable to conclude that the weaker performance of the older (and generally larger) trees at decadal and longer timescales is at least, in part, related to the greater likelihood that older trees will be affected by some disturbance event during their life than younger trees. Although the Figure 2d results represent a common period of analysis in the 20th century, disturbance trends in earlier parts of the older chronologies would still affect the chronology trends in this recent period (i.e. by biasing the fit of the detrending functions). Therefore, without addressing trend biases, sampling the largest (and perhaps oldest) trees will likely produce chronologies with poor climatic sensitivity at decadal and longer timescales. This presents a problem as the oldest trees are also the most valuable for studying longer-term climate. Furthermore, none of these strategies can guarantee a good chronology response in terms of climate signal. We must therefore ask the question, why is this the case, and does a reasonable approach exist for optimizing (maximizing) the climatic potential of the population sample? If disturbance is an important factor influencing climate response, then disturbance correction may be an appropriate strategy to improve calibration.

Previous studies have identified wind and windstorm damage as the dominant determinant of large scale severe disturbance in the Romanian Carpathians and to a lesser extent insect outbreaks and snow damage (e.g. Griffiths et al., 2014; Popa, 2008; Svoboda et al., 2014), which would account for the observed synchronous and temporally clustered nature of disturbance (Figure 3a) and the imprinting of disturbance trends in individual RW series on the mean chronologies (Figure 3b). There is also evidence that large scale severe windstorm events can impact the majority of trees over relatively large areas, as for example during the 2004 event in the Slovakian Tatra Mountains (Western Carpathians) which affected 12,000 ha of montane forest stands (e.g. Holeksa et al., 2016; Zielonka et al., 2010). The reduced range and more uniform trends expressed in individual PLOT chronologies, which more closely matched the mean (all 760 series) chronology after CID correction in Figure 3c compared to the pre-correction version in Figure 3b (particularly around the most prominent late 19th and early 20th century periods of growth release), suggests that CID correction produced individual PLOT sub-chronologies that more accurately approximate the larger-scale (regional population) chronology.

Compared to the lower mean correlation of the unfiltered pre-CID chronologies (Figure 3b, r = 0.28), correlations of the unfiltered post-CID chronologies (Figure 3c, r = 0.41) as well as the 1st differenced pre-CID and post-CID chronology versions (r = 0.45 and 0.49 respectively) were all considerably higher. This suggests that the high frequency climate signal in pre-CID chronologies was unaffected by the presence of disturbance trends and that the weaker correlations of the unfiltered pre-CID chronologies were related to the lower frequency trends, which was supported by the substantial degree of unfiltered post-CID correlation improvement (Figure 3c). Furthermore, the long term trend of the post-CID mean (all 760 series) chronology differed when compared to its pre-CID counterpart. Specifically, the most apparent changes included a reduction of index values affected by growth release in the first half of the 20th century and higher values before 1850 after correcting for non-climatic growth suppression trends. Taken together, the above evidence suggests that a disturbance-free chronology may not necessarily be achieved simply by collecting and averaging a very large number of series.

The improvement in post-CID chronology running correlations (Figure 3e) against both SIBIU and the longer CEU temperature series as well as the improved visual lower frequency trend agreement with these instrumental records (Figure 3f) suggests that the CID-corrected chronology better represented observed temperature trends. It should be pointed out that although CEU indicated warmer temperature conditions before the mid-19th century than suggested even by the post-CID chronology, early instrumental series (including those in central and eastern Europe) may contain a positive warm bias as a result of measurement practices and the lack of screen use before the mid / late

19th century (Böhm et al., 2010; Moberg et al., 2003). Hence, it is unclear whether the post-CID chronology indices were still too low or the instrumental record contained an early period warm bias.

The correlation and RMSE change results (Figure 4) indicate that, with one exception, all chronologies showed some degree of improvement after CID correction. Specifically, nearly all chronologies exhibited improved agreement (i.e. greater similarity) with the reference SIBIU instrumental temperature series expressed by a correlation increase and reduced RMSE. However, CID correction may not necessarily produce a substantial degree of improvement in all cases. In some instances this may be a result of applying CID to chronologies that already expressed a strong climate signal and did not exhibit any considerable degree of disturbance related trends (e.g. PLOT18 in Figure 4). In other cases, where only very limited improvement was observed in weakly correlating chronologies with temperature (e.g. PLOT1 in Figure 4), other unidentified factors (not necessarily related to disturbance) are likely responsible. In general, however, CID correction resulted in climate signal improvement for RW data, which is true, not only for location-based sampling, but also the other sampling strategies (Table 2 and 3). Spatially, it appears that a high severity disturbance event around the 1840s and possibly others in the subsequent decades mainly affected the northern and western slopes, whereas another event around the 1910s mostly affected the eastern slope. We hypothesize that this distinct spatial pattern and segregation of areas affected by disturbance in these two cases may point to windstorms as the most likely disturbance agent and that the spatial configuration of this pattern may be indicative of the spatially distinctive impact of wind disturbance in these two instances.

The PC analysis (Figure 5) demonstrates that even extracting the dominant modes of variability as PC scores, will not separate the climatic and non-climatic signals (i.e. this approach does not guarantee best achievable results when the influence of disturbance is present). Though these are the results of a local-scale analysis, it is conceivable that temporally common disturbance trends can be present in chronologies even over a larger region (e.g. due to wind storms or large-scale insect outbreaks). The inability to isolate the climate signal was expressed by the significant correlation of both PC1 and PC3 with temperature, but to a lesser degree also through their correlation with the disturbance chronology, which was mainly represented by PC2. After CID correction, a clearer separation of the climatic and non-climatic signals was achieved with PC analysis as indicated by the reduction from three dominant PCs to two and the increased correlation between PC2 and temperature. Importantly, however, though weaker (compared to pre-CID), the influence of the disturbance signal was reduced but not entirely removed by the CID procedure. This may be due to the relatively conservative threshold (3.29 sigma) applied in the identification of release events in order to minimize the likelihood of falsely identifying growth releases that are not disturbance related.

The parameter comparison for three sub-chronologies (PLOT 3, 7 and 10) in Figure 6 indicates that BI is not only the strongest temperature proxy but could potentially serve as a disturbance-free parameter, though further investigation in other locations and with additional species would be required to assess whether the decreased susceptibility of this parameter to disturbance is observed more generally. Kaczka and Czajka (2014) noted a similar (stronger than RW) summer temperature response of Norway spruce BI from Babia Góra in southern Poland. The importance of BI (and by extension maximum latewood density) to dendroclimatological research as a parameter that appears generally unaffected (or less affected) by disturbance and with a stronger climate signal is clearly emphasised by the evidence presented here. This may have implications for deriving chronologies free of disturbance with a stronger climatic signal as one possible way to by-pass the undesirable impact of disturbance on tree-ring data in dendroclimatic investigations. Furthermore, comparing RW and BI chronologies may represent an additional approach to the identification of disturbance trends in RW data.

A recent study by Rydval et al. (2016) demonstrated that disturbance related to anthropogenic activities (i.e. extensive logging) can induce growth trend biases in RW chronologies. The evidence presented herein demonstrates that <u>natural</u> disturbance can also potentially cause systematic chronology biases within closed-canopy forests. This can occur even if care is taken to select seemingly undisturbed sites as any evidence of disturbance occurring in the past (i.e. multiple decades or centuries ago) may have been erased from the landscape and may therefore no longer be visible at the time of sampling. By examining a very large number of samples, highly representative of the full stand population in this study, it is clear that the strength of the climate signal expressed in a chronology from a particular location can vary extensively and no sampling strategy can reliably ensure that the chronology produced from any set of collected RW samples will contain a well expressed climatic signal (i.e. the best achievable climate signal in RW data from a particular area). The development of chronologies which express a sufficiently strong common population signal (i.e. assessed using the widely applied EPS metric) can result in chronologies poorly correlated with climate even when the relationship between climate and chronologies from other sets of samples from the same area is considerably stronger. This can arise when non-climatic trends occur synchronously in those samples that make up a chronology.

The presupposition that collecting a large number of samples and avoiding disturbance-affected sampling locations can alleviate disturbance related biases in chronologies may be misleading because large-scale disturbances can affect whole stands and presumably even many stands in a region (e.g. due to wind disturbance or large-scale insect outbreaks). Nehrbass-Ahles (2014) performed an evaluation of sampling strategies, although it mainly assessed chronologies based on various sampling techniques in relation to the 'full population' and was also conducted in a managed stand that did not in fact display much climatic sensitivity. Such an approach, however, implicitly assumes that the population itself is unbiased in relation to its representation of the climate signal. Here we have demonstrated that the assumption of an unbiased population may not be justified. Evaluating chronologies in relation to the population (or rather a very large sample of the population) may therefore not represent a sound strategy in some cases as the possible influence of disturbance should also be taken into account. This finding provides some support for adopting strategies such as the careful selection (or screening) of samples at the local site level, or chronologies on the multi-site network scale, by assessing their climatic sensitivity in order to avoid including samples or chronologies significantly affected by disturbance in dendroclimatic analyses. Such screening practices have already been commonly applied in the development of reconstructions from large scale networks (e.g. Cook et al., 2013; Ljungqvist et al., 2016). Nevertheless, the use of methods such as CID may be preferable as this can reduce the risk of potential subjectivity and perhaps even expand the range of useable chronologies which may otherwise be deemed unsuitable for dendroclimatic analysis.

Although this study demonstrates this issue only at a single location, there is potential for systematic disturbance to affect RW chronologies in virtually any closed canopy forest ecosystem and such a possibility cannot be dismissed *a priori*. The issues highlighted and discussed here may for example directly affect calibration strength of reconstructions as well as the possibility of making inaccurate inferences about past climatic conditions from RW-based reconstructions that may include disturbance related biases. It is important to be able to perform some assessment of possible disturbance effects on RW chronologies because assessing the fidelity of reconstructed climate estimates before the instrumental period is difficult. We therefore recommend that all future dendrochronological studies investigating medium to low frequency climatic trends should perform some form of disturbance assessment and that the CID method (Druckenbrod et al., 2013; Rydval et al., 2016) represents a reasonable approach.

CONCLUSION

In this study, we have demonstrated that natural disturbance events can act as agents which significantly and systematically affect tree growth, subsequently biasing mid- to long-term RW chronology trends. These disturbance trends cannot be removed using conventional detrending approaches without also removing lower frequency climatic information. In closed canopy forests, the oldest (and dendroclimatologically most valuable) trees are more likely to contain an embedded disturbance response. It is not possible to ensure that this response can be factored out or minimized simply by adopting a subjective sampling strategy or relying on a very large sample size (with respect to both trees and sites). Furthermore, sampling trees across a landscape may produce a record with a complex range of disturbance histories rather than reducing the disturbance signals. This important finding highlights the need to develop site selection and sampling approaches for closed-canopy forests that are very different from those developed by Fritts (1976) for open-canopy forests. More specifically, it is imperative to develop better methods to disentangle disturbance and climate signals.

Disturbance detection techniques could be used, at a minimum, to identify and assess the effects of disturbance on RW chronologies and (if replication permits) exclude subsets substantially affected by such trends which would therefore represent a poorer expression of longer term climatic variability. This also provides justification for the application of approaches such as data screening in order to exclude subsets of larger datasets, which are weakly correlated with climate, from climatic analyses. An alternative approach would include the utilization of some sort of disturbance correction procedure (e.g. CID) to improve the expression of the climate signal in disturbance affected RW series. Finally, other tree-ring parameters, such as BI (or maximum latewood density), which may be less prone to the effects of disturbance and often express a stronger climate signal than RW (Wilson et al. 2016), could also be developed.

The findings of this study are broadly applicable and of relevance to RW chronologies from closed canopy stands. Additional larger scale investigations including various species from other locations would be beneficial in assessing the relevance of our findings. Certainly, consideration should be given to the possibility of disturbance related trends affecting medium to low frequency growth trends in RW chronologies. We therefore recommend that some form of evaluation of this potential effect should be performed as part of any dendrochronological research utilizing RW data to investigate climatic trends as it may be possible to reduce this limitation and improve the expression of the climate signal in such data.

ACKNOWLEDGEMENTS

The study was supported by the institutional project MSMT (CZ.02.1.01/0.0/0.0/16_019/0000803) and the Czech Ministry of Education (Project INTER-COST no. LCT17055). We thank the Călimani National Park authorities, especially E. Cenuşă and local foresters, for administrative support and assistance in the field.

REFERENCES

Anchukaitis KJ, Wilson R, Briffa KR et al. (2017) Last millennium Northern Hemisphere summer temperatures from tree rings: Part II, spatially resolved reconstructions. *Quaternary Science Reviews* 163: 1-22.

Attiwill PM (1994) The disturbance of forest ecosystems: the ecological basis for conservative management. *Forest Ecology and Management* 63(2): 247-300.

Björklund JA, Gunnarson BE, Seftigen K et al. (2014a) Blue intensity and density from northern Fennoscandian tree rings, exploring the potential to improve summer temperature reconstructions with earlywood information. *Climate of the Past* 10(2): 877-885.

Björklund J, Gunnarson BE, Seftigen K et al. (2014b) Using adjusted Blue Intensity data to attain high-quality summer temperature information: A case study from Central Scandinavia. *Holocene* 25(3): 547-556.

Böhm R, Jones PD, Hiebl J et al. (2010) The early instrumental warm-bias: a solution for long central European temperature series 1760–2007. *Climatic Change* 101(1-2): 41-67.

Box GEP and Jenkins GM (1970) *Time series analysis: forecasting and control*. San Francisco, CA: Holden-Day, 553 pp.

Box GE and Tiao GC (1975) Intervention analysis with applications to economic and environmental problems. *Journal of the American Statistical Association* 70(349): 70-79.

Briffa K and Melvin T (2011) A Closer Look at Regional Curve Standardization of Tree-Ring Records: Justification of the Need, a Warning of Some Pitfalls, and Suggested Improvements in Its Application. In: Hughes MK, Swetnam TW and Diaz HF (eds) *Dendroclimatology: progress and prospects*. Dordrecht: Springer, pp. 113-145.

Briffa KR, Jones PD, Schweingruber FH et al. (1996) Tree-ring variables as proxy-climate indicators: problems with low-frequency signals. In: Jones PD, Bradley S and Jouzel J (eds) *Climatic Variations and Forcing Mechanisms of the Last 2000 Years*. Berlin Heidelberg: Springer, pp. 9-41.

Carrer M and Urbinati C (2004) Age-dependent tree-ring growth responses to climate in Larix decidua and Pinus cembra. *Ecology* 85(3): 730-740.

Cherubini P, Dobbertin M and Innes JL (1998) Potential sampling bias in long-term forest growth trends reconstructed from tree rings: a case study from the Italian Alps. *Forest Ecology and Management* 109(1-3): 103-118.

Cook ER (1985) *A Time Series Analysis Approach to Tree Ring Standardization*. PhD Thesis, University of Arizona, Tucson, AZ, USA.

Cook ER and Kairiukstis LA (1990) *Methods of Dendrochronology: applications in the environmental sciences*. Dordrecht: Kluwer Academic Publishers, 394 pp.

Cook ER and Krusic PJ (2005) *Program ARSTAN: a tree-ring standardization program based on detrending and autoregressive time series modeling, with interactive graphics*. Lamont-Doherty Earth Observatory, Columbia University, Palisades, NY.

Cook ER and Peters K (1981) The smoothing spline: a new approach to standardizing forest interior tree-ring width series for dendroclimatic studies. *Tree-Ring Bulletin* 41: 45-53.

Cook ER and Peters K (1997) Calculating unbiased tree-ring indices for the study of climatic and environmental change. *Holocene* 7(3): 361-370.

Cook BI, Anchukaitis KJ, Touchan R et al. (2016) Spatiotemporal drought variability in the Mediterranean over the last 900 years. *Journal of Geophysical Research: Atmospheres* 121(5). DOI:10.1002/2015JD023929.

Cook ER, Briffa KR, Meko DM et al. (1995) The 'segment length curse' in long tree-ring chronology development for palaeoclimatic studies. *Holocene* 5(2): 229-237.

Cook ER, Krusic PJ, Anchukaitis KJ et al. (2013) Tree-ring reconstructed summer temperature anomalies for temperate East Asia since 800 CE. *Climate Dynamics* 41(11-12): 2957-2972.

Cook ER, Seager R, Kushnir Y et al. (2015) Old World megadroughts and pluvials during the Common Era. *Science Advances* 1(10). DOI:10.1126/sciadv.1500561.

D'Amato AW and Orwig DA (2008) Stand and landscape-level disturbance dynamics in old-growth forests in Western Massachusetts. *Ecological Monographs* 78(4): 507–522.

D'Arrigo R, Wilson R and Jacoby G (2006) On the long-term context for late twentieth century warming. *Journal of Geophysical Research: Atmospheres* 111(D3). DOI:10.1029/2005JD006352.

Druckenbrod DL (2005) Dendroecological reconstructions of forest disturbance history using time-series analysis with intervention detection. *Canadian Journal of Forest Research* 35(4): 868-876.

Druckenbrod DL, Pederson N, Rentch J et al. (2013) A comparison of times series approaches for dendroecological reconstructions of past canopy disturbance events. *Forest Ecology and Management* 302: 23-33.

Düthorn E, Holzkämper S, Timonen M et al. (2013) Influence of microsite conditions on tree-ring climate signals and trends in central and northern Sweden. *Trees* 27(5): 1395-1404.

Düthorn E, Schneider L, Konter O et al. (2015) On the hidden significance of differing micro-sites on tree-ring based climate reconstructions. *Silva Fennica* 49(1). DOI:10.14214/sf.1220.

Esper J, Niederer R, Bebi P et al. (2008) Climate signal age effects — evidence from young and old trees in the Swiss Engadin. *Forest Ecology and Management* 255(11): 3783-3789.

Fish T, Wilson R, Edwards C et al. (2010) Exploring for senescence signals in native scots pine (Pinus sylvestris L.) in the Scottish Highlands. *Forest Ecology and Management* 260(3): 321-330.

Fritts HC (1976) *Tree rings and climate*. London: Academic Press, 567 pp.

Griffiths P, Kuemmerle T, Baumann M et al. (2014) Forest disturbances, forest recovery, and changes in forest types across the Carpathian ecoregion from 1985 to 2010 based on Landsat image composites. *Remote Sensing of Environment* 151: 72-88.

Gunnarson BE, Josefsson T, Linderholm HW et al. (2012) Legacies of pre-industrial land use can bias modern tree-ring climate calibrations. *Climate Research* 53(1): 63-76.

Helama S, Lindholm M, Timonen M et al. (2004) Detection of climate signal in dendrochronological data analysis: a comparison of tree-ring standardization methods. *Theoretical and Applied Climatology* 79(3-4): 239-254.

Holeksa J, Zielonka T, Żywiec M et al. (2016) Identifying the disturbance history over a large area of larch–spruce mountain forest in Central Europe. *Forest Ecology and Management* 361: 318-327.

Hughes MK (2011) Dendroclimatology in High-Resolution Paleoclimatology. In: Hughes MK, Swetnam TW and Diaz HF (eds) *Dendroclimatology: progress and prospects*. Dordrecht: Springer, pp. 17-34.

Kaczka RJ and Czajka B (2014) Intensywność odbicia światła niebieskiego jako nowy nośnik informacji w badaniach dendrochronologicznych. *Studia i Materiały Centrum Edukacji Przyrodniczo-Leśnej w Rogowie* 16(40): 274-282.

Kulakowski D and Veblen TT (2002) Influences of fire history and topography on the pattern of a severe wind blowdown in a Colorado subalpine forest. *Journal of Ecology* 90(5): 806–819.

Larsson L (2015) CooRecorder and Cdendro programs of the CooRecorder/Cdendro package version 7.8. Available at: http://www.cybis.se/forfun/dendro/ (accessed 10 October 2015).

Ljungqvist FC, Krusic PJ, Sundqvist HS et al. (2016) Northern Hemisphere hydroclimate variability over the past twelve centuries. *Nature* 532(7597): 94-98.

Luterbacher J, Werner JP, Smerdon JE et al. (2016) European summer temperatures since Roman times. *Environmental Research Letters* 11(2). DOI: 10.1088/1748-9326/11/2/024001.

McCarroll D, Loader NJ, Jalkanen R et al. (2013) A 1200-year multiproxy record of tree growth and summer temperature at the northern pine forest limit of Europe. *Holocene* 23(4): 471-484.

McCarroll D, Pettigrew E, Luckman A et al. (2002) Blue reflectance provides a surrogate for latewood density of high-latitude pine tree rings. *Arctic, Antarctic, and Alpine Research* 34(4): 450-453.

Melvin TM and Briffa KR (2008) A “signal-free” approach to dendroclimatic standardisation. *Dendrochronologia* 26(2): 71-86.

Melvin TM, Grudd H and Briffa KR (2013) Potential bias in ‘updating’tree-ring chronologies using regional curve standardisation: Re-processing 1500 years of Torneträsk density and ring-width data. *Holocene* 23(3): 364-373.

Mérian P, Bert D and Lebourgeois F (2013) An approach for quantifying and correcting sample size-related bias in population estimates of climate-tree growth relationships. *Forest Science* 59(4): 444-452.

Moberg A, Alexandersson H, Bergström H et al. (2003) Were southern Swedish summer temperatures before 1860 as warm as measured?. *International Journal of Climatology* 23(12): 1495-1521.

Nehrbass-Ahles C, Babst F, Klesse S et al. (2014) The influence of sampling design on tree-ring-based quantification of forest growth. *Global Change Biology* 20(9): 2867-2885.

Osborn TJ, Briffa KR and Jones PD (1997) Adjusting variance for sample size in tree-ring chronologies and other regional mean timeseries. *Dendrochronologia* 15(89): 89-99.

Popa I (2008) Windthrow risk management. Results from Romanian forests. In: *Forest disturbances and effects on carbon stock: The non-permanence issue* (eds Anfodillo T, Dalla Valle E and Valese E), San Vito di Cadore, Italy, 9-12 June 2008,pp. 77-88. Padua: Università di Padova.

Popa I and Kern Z (2009) Long-term summer temperature reconstruction inferred from tree-ring records from the Eastern Carpathians. *Climate Dynamics* 32(7-8): 1107-1117.

Primicia I, Camarero JJ, Janda P et al. (2015) Age, competition, disturbance and elevation effects on tree and stand growth response of primary Picea abies forest to climate. *Forest Ecology and Management* 354: 77-86.

Rydval M, Druckenbrod DL, Anchukaitis KJ et al. (2016) Detection and removal of disturbance trends in tree-ring series for dendroclimatology. *Canadian Journal of Forest Research* 46(3): 387-401.

Rydval M, Larsson LÅ, McGlynn L et al. (2014) Blue Intensity for dendroclimatology: Should we have the blues? Experiments from Scotland. *Dendrochronologia* 32(3): 191-204.

Sidor CG, Popa I, Vlad R et al. (2015) Different tree-ring responses of Norway spruce to air temperature across an altitudinal gradient in the Eastern Carpathians (Romania). *Trees* 29(4): 985-997.

SPSS (2011) IBM SPSS statistics for Windows, version 20.0. New York: IBM Corp.

Stokes MA and Smiley TL (1968) *An introduction to tree-ring dating*. Chicago: University of Chicago Press, 73 pp.

Svoboda M, Janda P, Bače R et al. (2014) Landscape-level variability in historical disturbance in primary Picea abies mountain forests of the eastern Carpathians, Romania. *Journal of Vegetation Science* 25(2): 386-401.

Vaganov EA, Hughes MK, Shashkin AV et al. (2006)*Growth Dynamics of Conifer Tree Rings: Images of Past and Future Environments*. Berlin Heidelberg: Springer, 354 pp.

Valtera M, Šamonil P and Boublík K (2013) Soil variability in naturally disturbed Norway spruce forests in the Carpathians: bridging spatial scales. *Forest Ecology and Management* 310: 134-146.

Warren WG (1980) On removing the growth trend from dendrochronological data. *Tree-Ring Bulletin* 40: 35-44.

Wigley TML, Briffa KR and Jones PD (1984) On the average of correlated time series, with applications in dendroclimatology and hydrometeorology. *Journal of Climate and Applied Meteorology* 23(2): 201-213.

Wilson R, Anchukaitis K, Briffa KR et al. (2016) Last millennium northern hemisphere summer temperatures from tree rings: Part I: The long term context. *Quaternary Science Reviews* 134(1): 1-18.

Wilson R, Rao R, Rydval M et al. (2014) Blue Intensity for dendroclimatology: The BC blues: A case study from British Columbia, Canada. *Holocene* 24: 1428-1438.

Zielonka T, Holeksa J, Fleischer P et al. (2010) A treering reconstruction of wind disturbances in a forest of the Slovakian Tatra Mountains, Western Carpathians.*Journal of Vegetation Science* 21(1): 31–42.

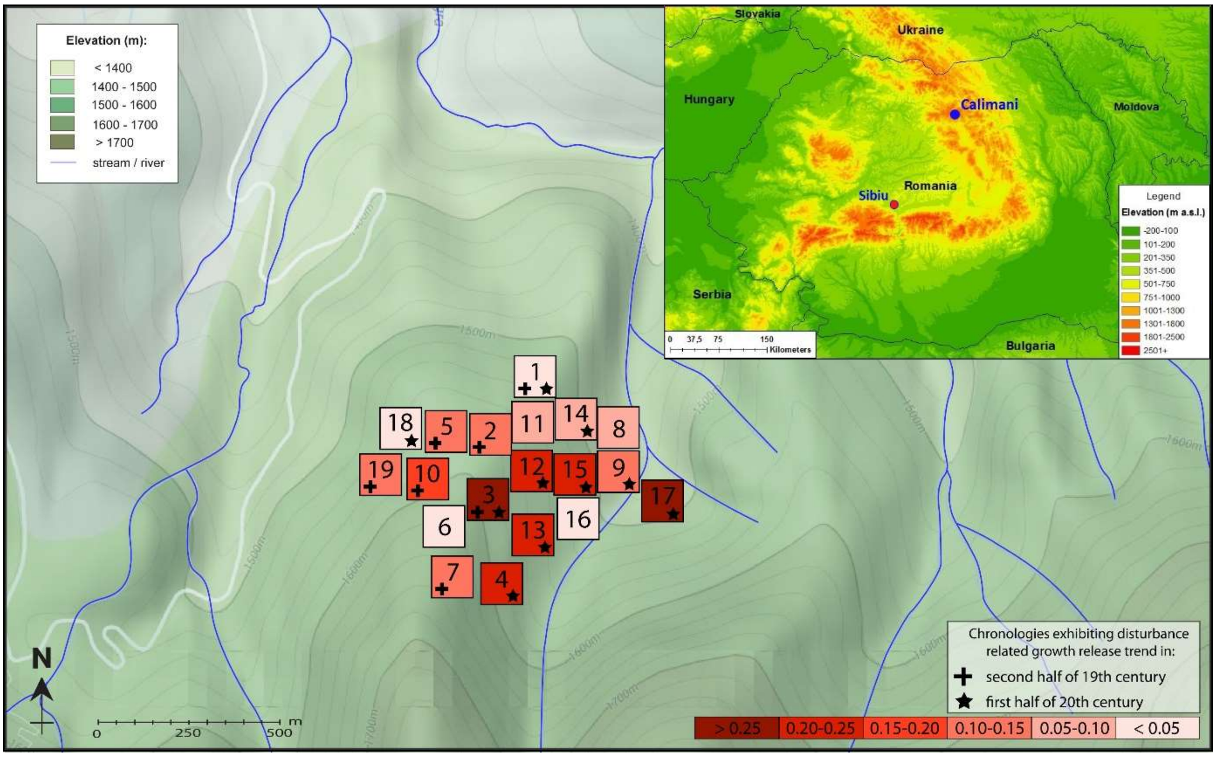

Figure 1: Site location and approximate distribution of sampling plots in Calimani National Park, Romania. Red shading represents post-disturbance correction correlation increase* of plot-based (PLOT) chronologies (see Table 1 for details) against June-July mean instrumental temperatures for the full length of chronologies – same representation as Figure 4C. (*note that chronology PLOT-16 shows a slight correlation decrease after disturbance correction).

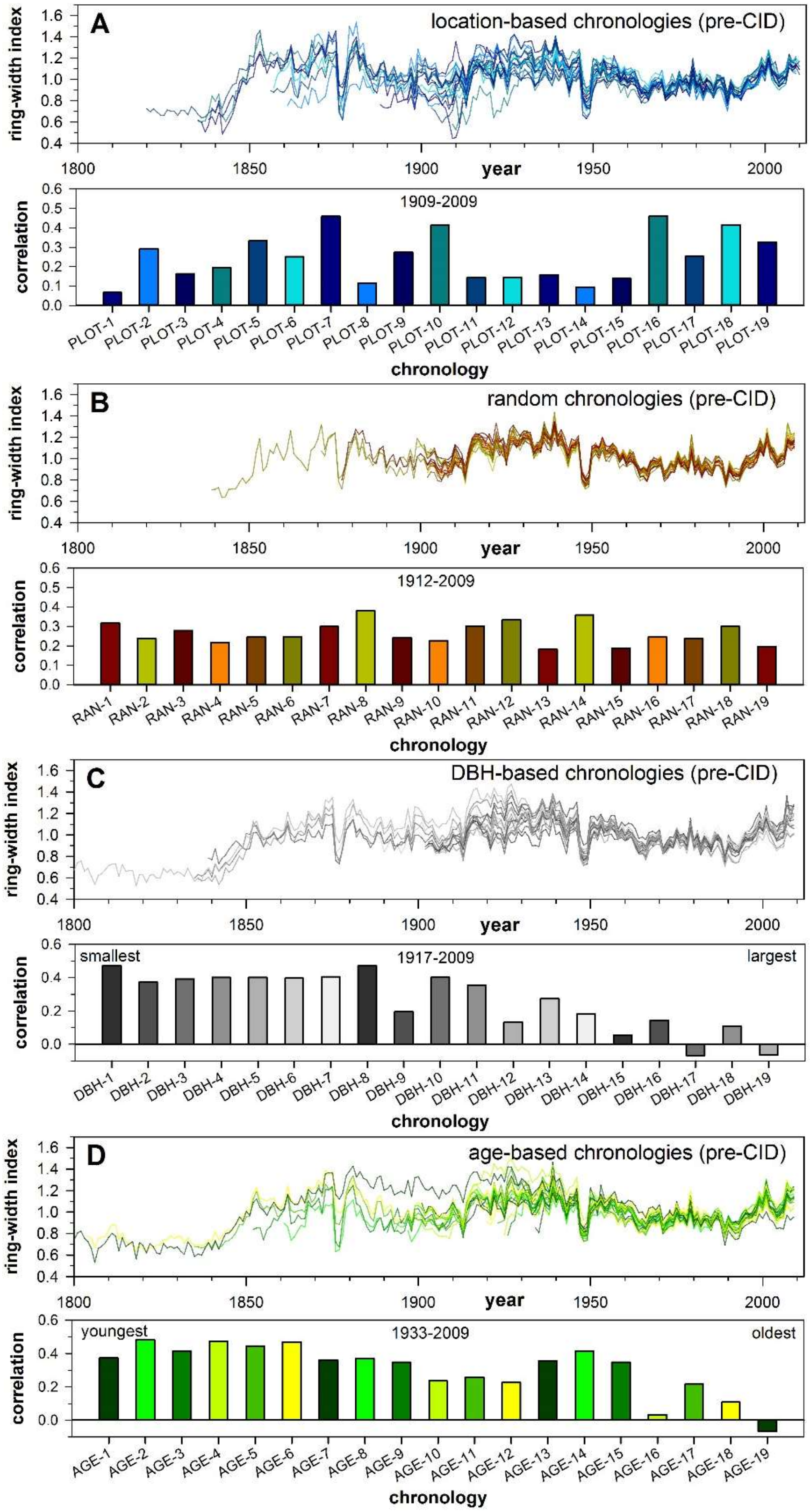

Figure 2: Chronology plots and correlations with Jun-Jul mean temperatures from Sibiu for four 'sampling' methods including grouping according to (A) sample location (PLOT), (B) random sample selection (RAN), (C) diameter at breast height (DBH) (D) and recruitment age (AGE) – see Table 1 for additional details. Each chronology was truncated in the year where expressed population signal dropped below 0.85. (pre-CID indicates that chronologies were developed with series before correcting for disturbance trends using the Curve Intervention Detection method)

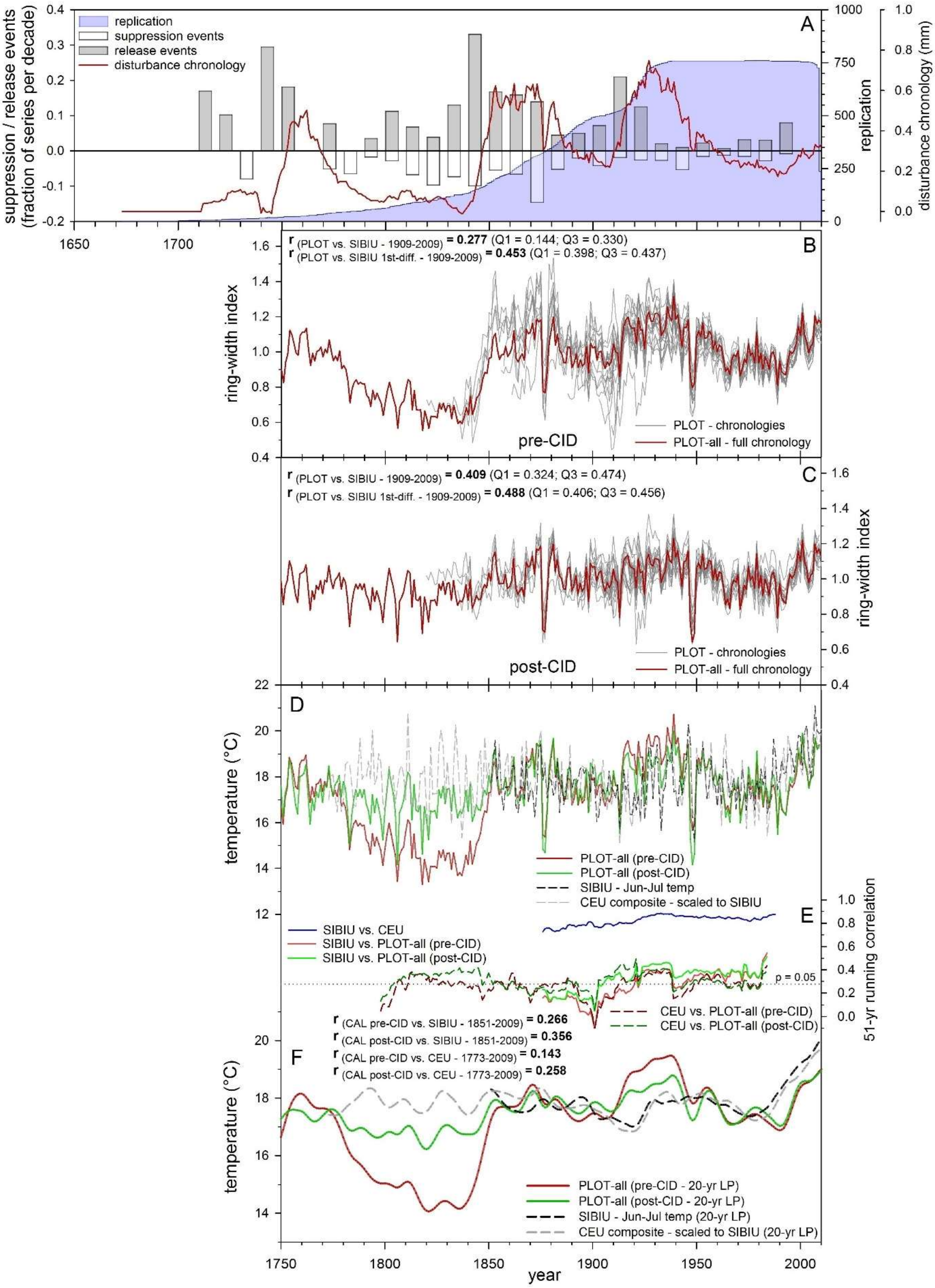

Figure 3: (A) Summary of Calimani disturbance history from Curve Intervention Detection (CID) analysis; (B) chronologies before disturbance correction (pre-CID) and (C) after disturbance correction (post-CID) and (D) pre-CID/post-CID chronologies with Jun-Jul temperatures from Sibiu (SIBIU) and the longer central/east Europe (CEU) Jun-Jul regional composite temperature series; (E) 51-year running correlations between instrumental and ring-width chronologies in (D); (F) as in (D) except smoothed with a 20 year low-pass Gaussian filter.

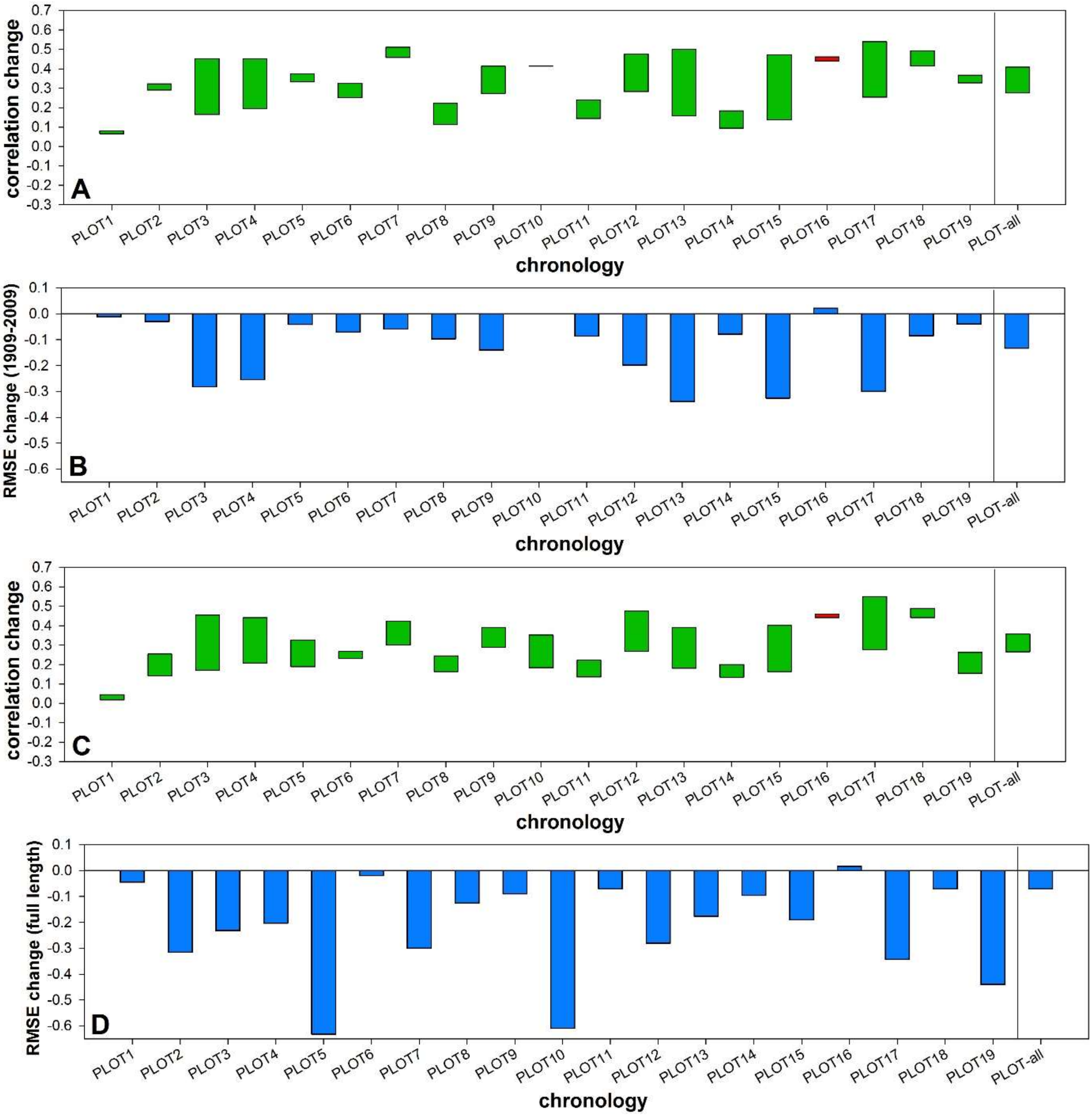

Figure 4: Comparing the (A, C) change in correlation and (B, D) root-mean-square error change of Calimani plot-based (PLOT) chronologies before disturbance correction (pre-CID) vs. after disturbance correction (post-CID) in relation to instrumental temperature data from Sibiu for the (A, B) 1909-2009 period and (C, D) full chronology length (max. back to 1851). (The green colour in A and C indicates the size of the correlation increase after disturbance correction whereas red colour (only PLOT16) indicates a correlation decrease.)

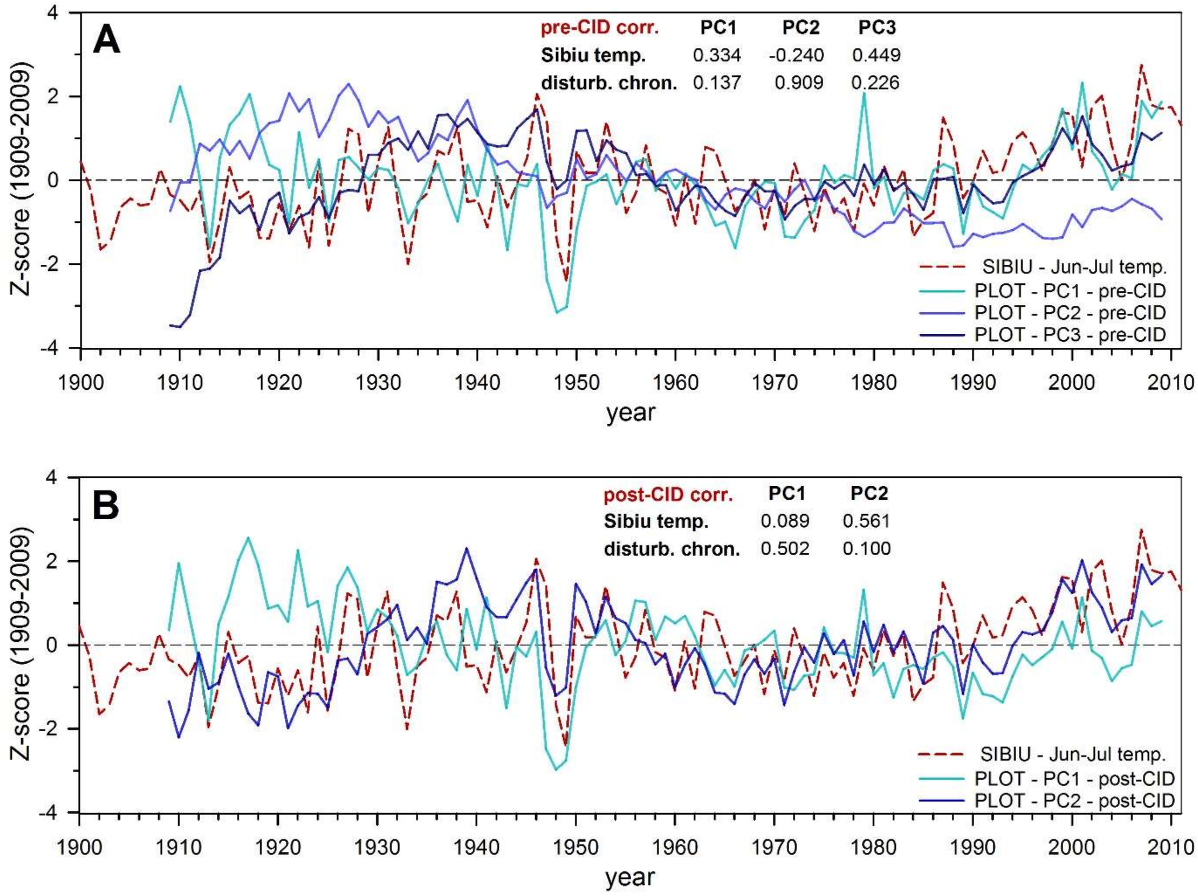

Figure 5: Amplitudes of the dominant principal components (PCs) from chronologies developed (A) before disturbance correction (pre-CID) and (B) after disturbance correction (post-CID), and their correlation with instrumental temperatures from Sibiu and the disturbance chronology in Figure 3A. (Scatterplots of significant relationships ($p < 0.01$) between the PCs and the disturbance chronology / Sibiu temperatures are represented in supplementary figure S5).

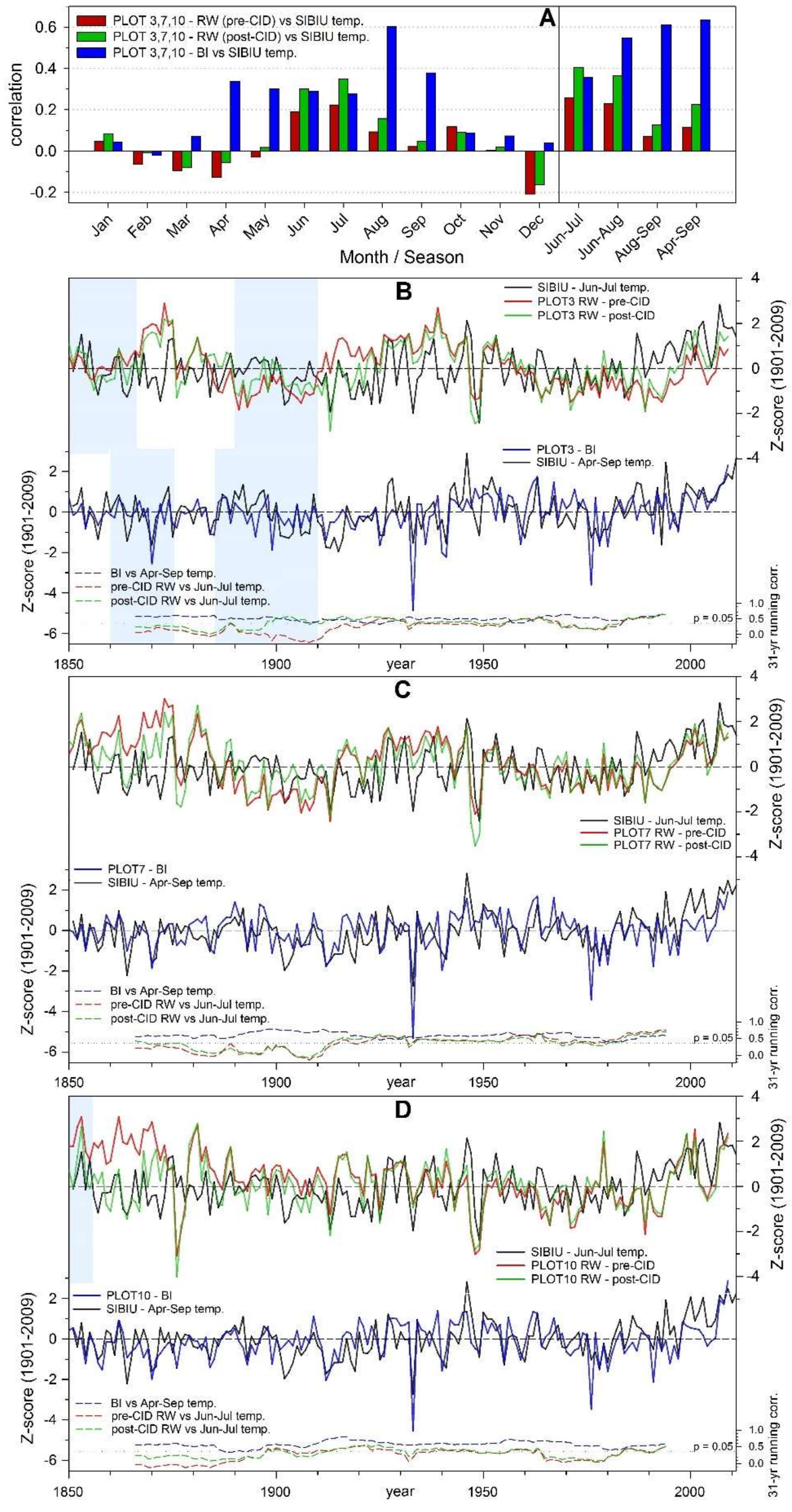

Figure 6: Comparison of the PLOT-3, PLOT-7 and PLOT-10 blue intensity (BI) and ring width (RW) chronologies developed before (pre-CID) and after (post-CID) disturbance correction with instrumental temperatures from Sibiu (SIBIU) over the 1851-2009 period showing (A) the combined correlation response of the Calimani chronologies against SIBIU temperatures; and the time-series of the RW and BI chronologies together with Jun-Jul and Apr-Sep SIBIU mean temperature respectively for (B) PLOT-3, (C) PLOT-7 and (D) PLOT-10. (Highlighted periods indicate where expressed population signal is < 0.85.)

Supplementary figures

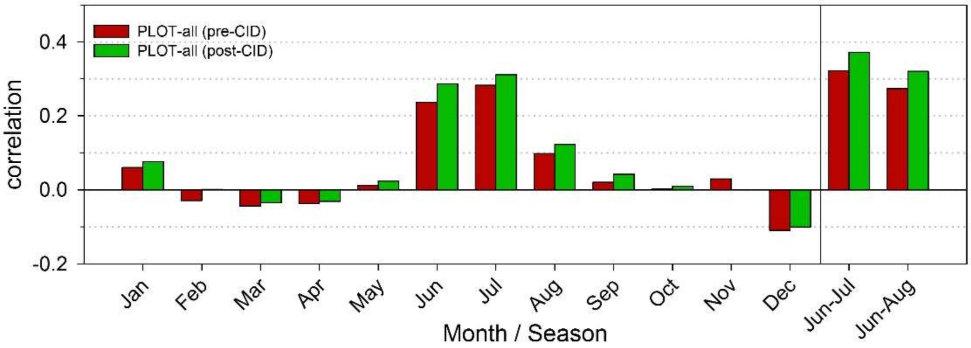

Figure S1: Correlation response of chronologies composed of all 760 series from Calimani (PLOT-all) before (pre-CID) and after (post-CID) disturbance correction against mean monthly and seasonal temperatures from Sibiu for the 1851-2011 period.

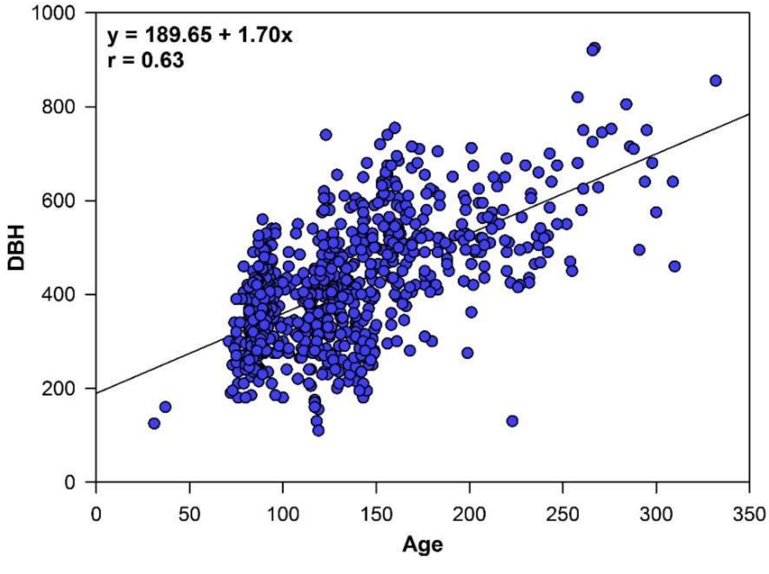

Figure S2: Relationship between estimated tree age and diameter at breast height (DBH).

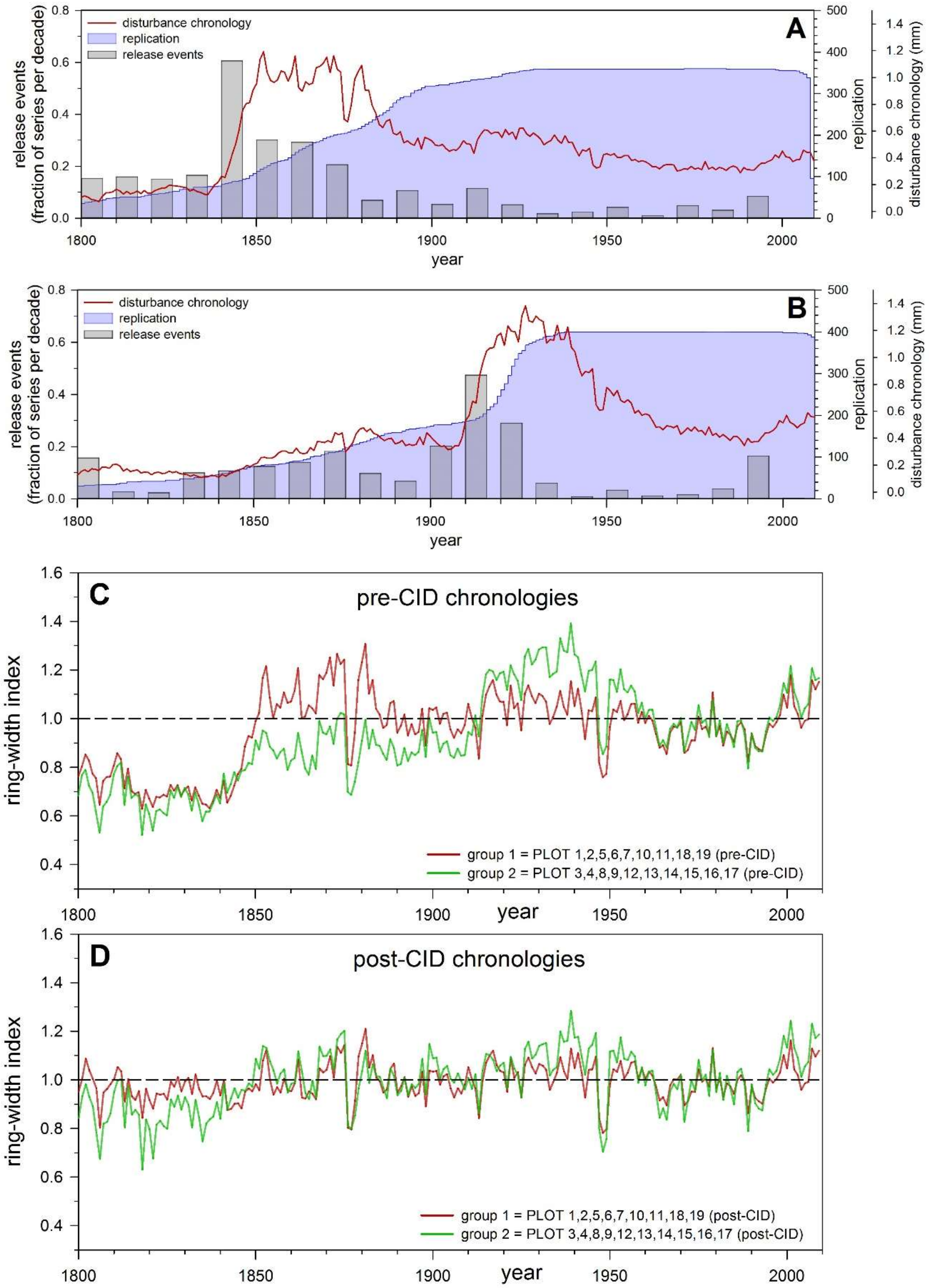

Figure S3: Summary of Calimani disturbance history from Curve Intervention Detection (CID) analysis (A) using series from plots from the northwest part of the stand (Figure 1 - PLOT 1, 2 , 5, 6, 7, 10, 11, 18, 19) predominantly affected by disturbance in the mid-19th century and (B) from the southeast part for the stand (Figure 1 – PLOT 3, 4, 8, 9, 12, 13, 14, 15, 16, 17) predominantly affected by disturbance in the early 20th century. The before disturbance correction (pre-CID) and after disturbance correction (post-CID) chronologies of these two spatial groups are presented in (C) and (D) respectively.

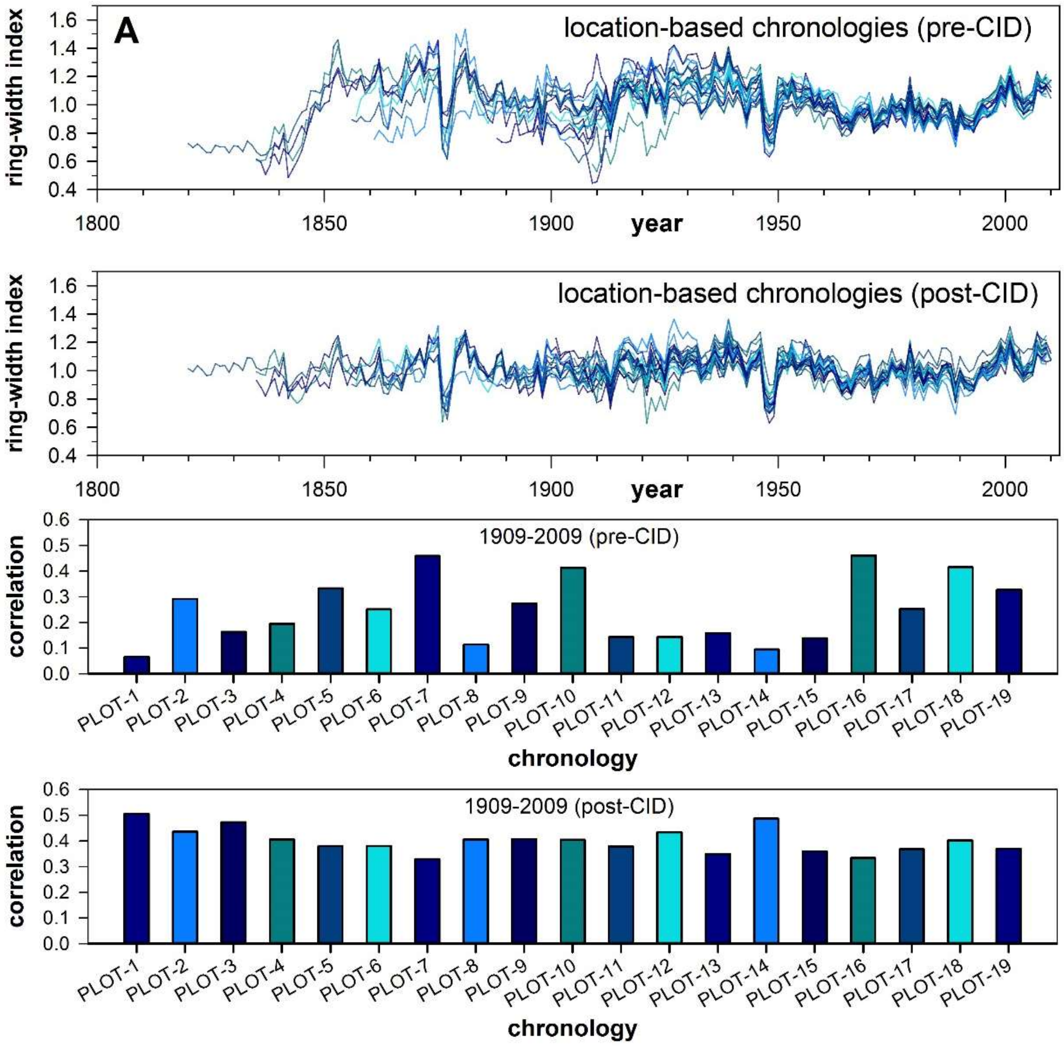

Figure S4: Before disturbance correction (pre-CID) and after disturbance correction (post-CID) chronology plots and correlations with Jun-Jul mean temperatures from Sibiu for four 'sampling' methods including grouping according to (A) sample location (PLOT), (B) random sample selection (RAN), (C) diameter at breast height (DBH) (D) and recruitment age (AGE) – see Table 1 for additional details. Each chronology was truncated in the year where expressed population signal dropped below 0.85.

Figure S4 – continued

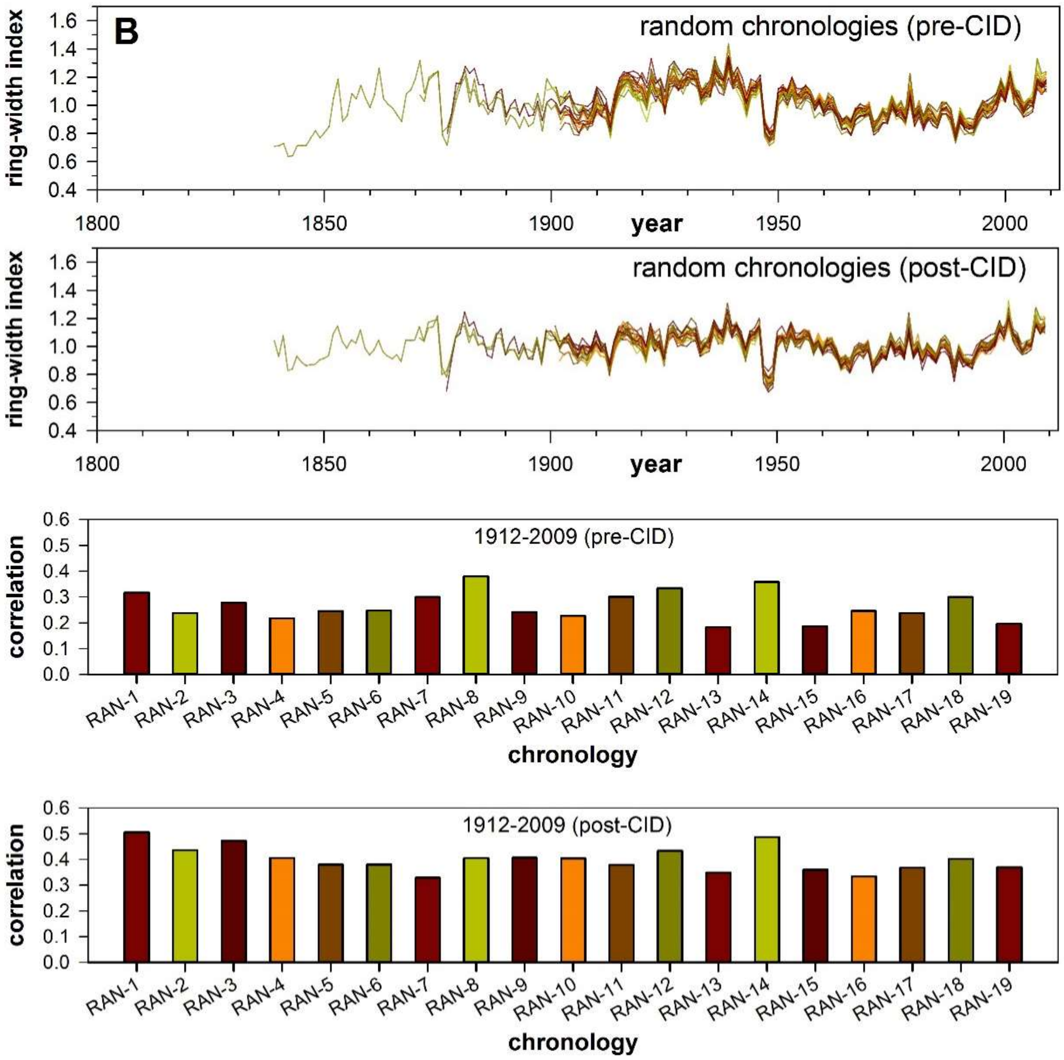

Figure S4 – continued

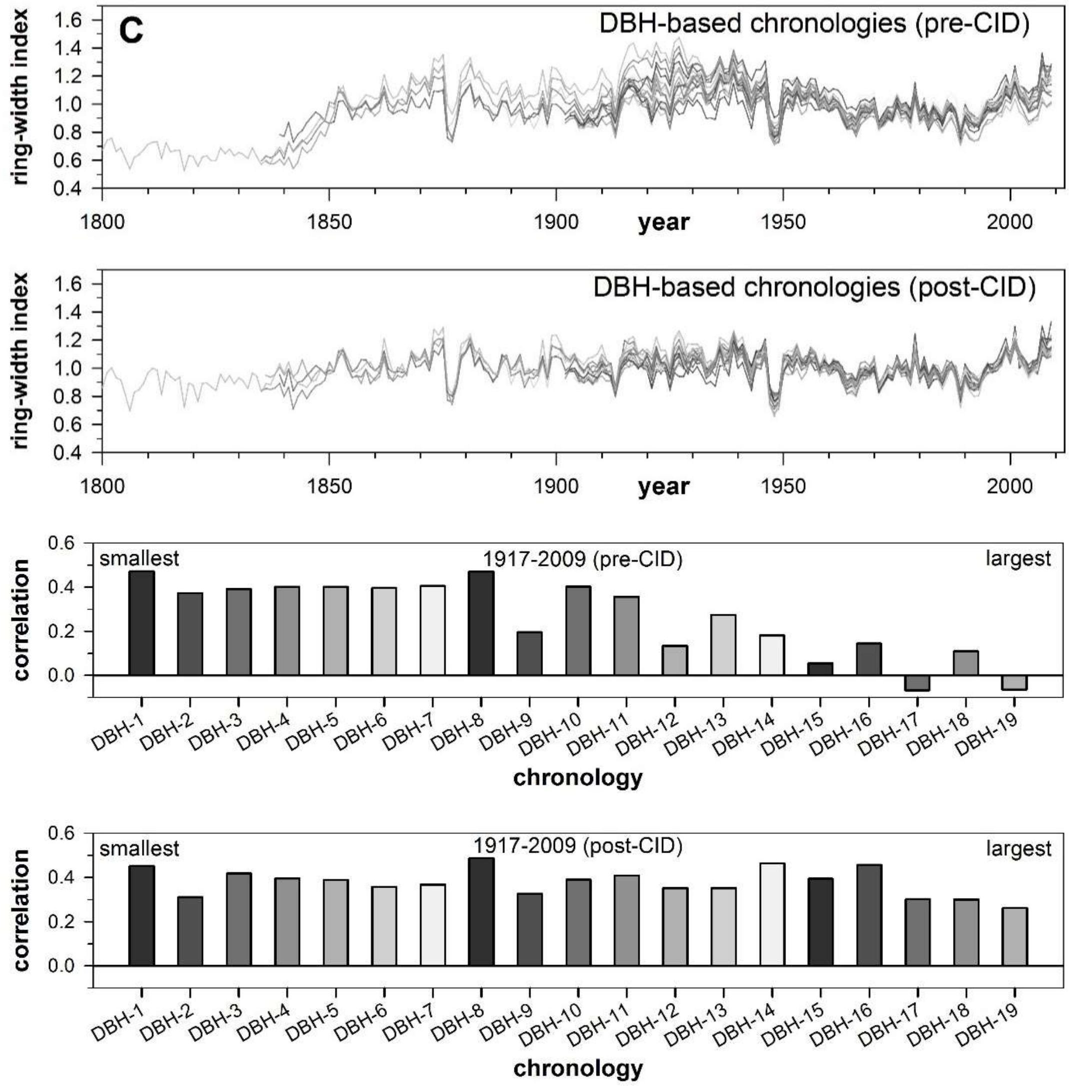

Figure S4 – continued

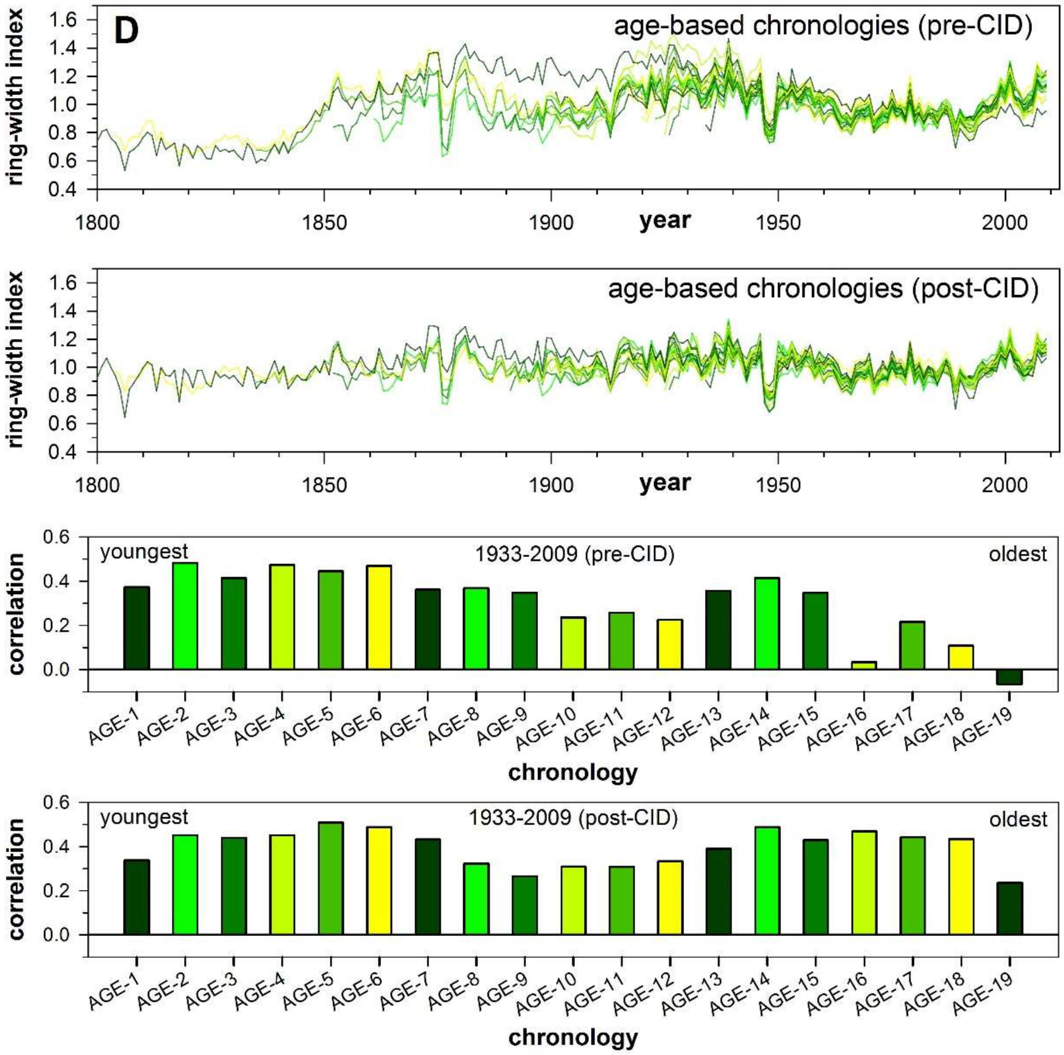

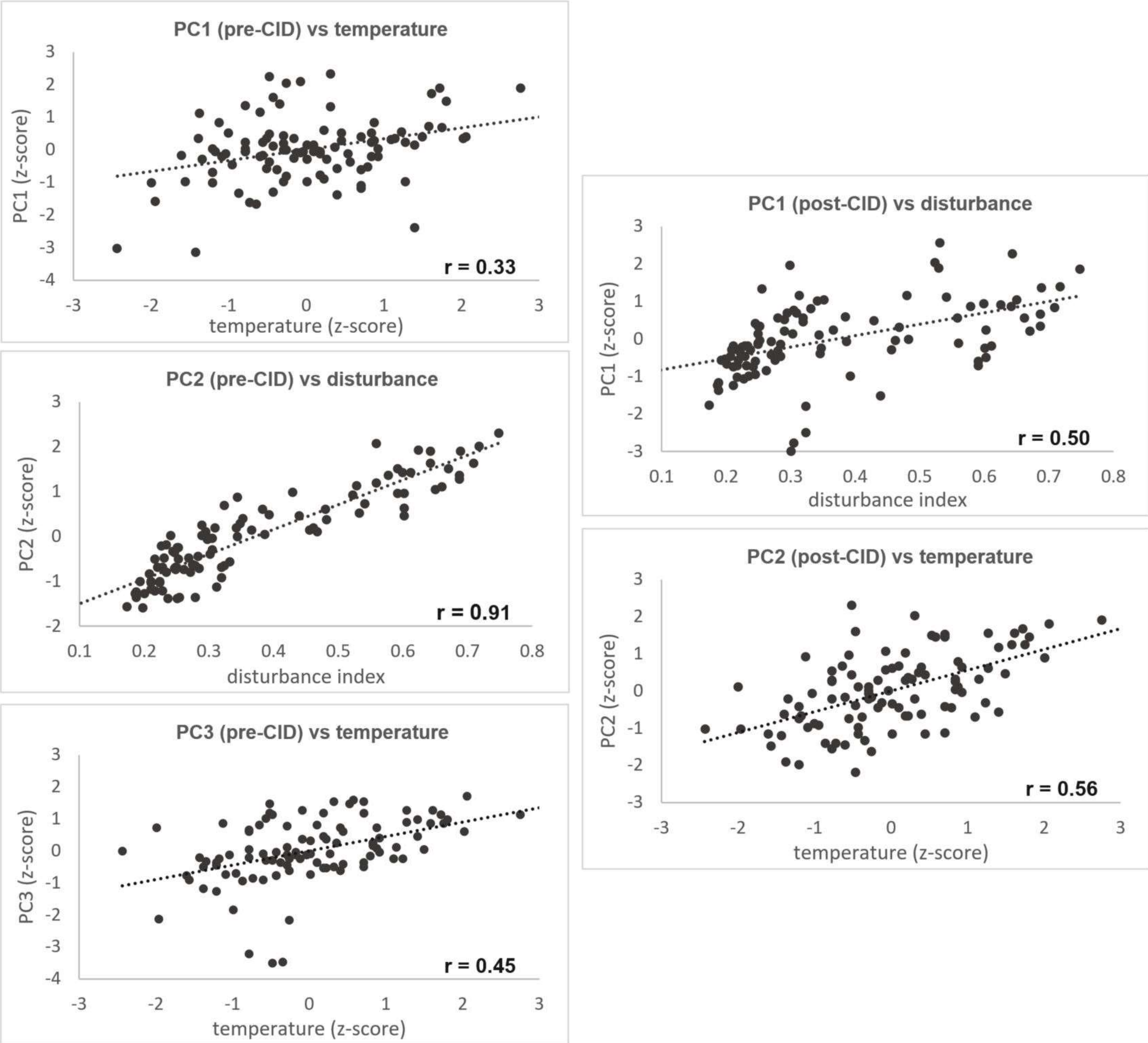

Figure S5: Scatterplots of significant relationships ($p < 0.01$) between the disturbance chronology in Figure 3A / Jun-July average Sibiu temperatures and amplitudes of the dominant principal components (PCs) from chronologies developed before disturbance correction (pre-CID) and after disturbance correction (post-CID).

Curve Intervention Detection (CID) Matlab code

```
function [ymn,varyh,df,w,ybar,se]=bisqmean_CID(y)
%
% Biweight mean for a vector of numbers.
% Last revised 2011-7-09
% Revised by Daniel Druckenbrod 2012-1-11
%
% Source:  Mosteller and Tukey (1977, p. 205, p 351-352)
%       Cook and  Kairiukstis (1990, p. 125-126)
%
%
%***************  INPUT ************************
%
% y  (? x 1)r  vector of data -- say, indices for ? cores in a year
%
%
%*******************  OUTPUT ***********************
%
% ymn  (1 x 1)r  biweight mean
% varyh  (1 x 1)r   asymptotic standard dev of biweight mean - p. 208,
%       third eqn from top of page
% df  (1x1)r degrees of freedom
% w  (? x 1)r  final weights on values in y
% ybar  (1 x 1)r arithmetic mean corresponding to ymn
% se  (1 x 1)r  standard error of ybar
%
%*******************  NOTES ********************
%
% ybar and se just included in debugging  to double check
% on closeness of ybar to ymn, se to sqrt(varyh)
%
%*******************************************************************


sens = 0.001;  % hard coded theshold of sensitivity for stopping
iterat
nits = 100;  % max number of allowed iterations

[n,ny]=size(y);
if ny > 1;
    error('y should be a vector')
end

if any(isnan(y));
    error('y not permitted to have NaNs');
end;

if n<6; % if fewer than 6 sample size, use median
    ymn = median(y);
    w=[];
    ybar=mean(y);
    se= sqrt(var(y)/n); % standard error of mean
    df=[];
    varyh=NaN;
    return;
end;
```

```
ww = 1/n; % weight for even average
ybar = mean(y); % arith mean
%ybar=median(y);
se= sqrt(var(y)/n); % standard error of mean

nz=0;
ymn = ybar; % initial biweight mean as arith mean

for i = 1: nits;  % iterate max of nits times
    ymnold = ymn;  % store old value of mean
    e = y-ymn; % deviations from mean
    S = median(abs(e));  % median abs deviation
    u = e / (6*S);  % scaled deviations

    w = (1 - u.^2).^2;  % compute weights
    L1 = abs(u)>=1; % flag huge errors
    L1s = sum(L1);
    if L1s>0
        nz=0;
        nz= nz(ones(L1s,1),:);
        w(L1)=nz;  % set weights on those obs to zero
    end
    w = w / sum(w); % adjust weights to sum to 1.0

    ymn = sum(w .* y); % compute biweight mean


    % Variance of estimate of biweight mean
    ui= e / (9*S);
    L2 = ui>1;
    ui(L2)=[];
    z =y(~L2);
    nz = length(z);
    nom1 = (z - ymn) .^2;
    nom2 = (1-ui .^2) .^4;
    nom = sum(nom1 .* nom2);

    den1 = sum((1-ui .^2) .* (1-5*ui .^2));

    varyh_hoaglin=(n^0.5)*(nom^0.5)/den1; % Dan: p. 417 3rd equation
    den2 = -1 + sum ((1-ui .^2) .* (1-5*ui .^2));
    % varyh = nom / (den1*den2);  % variance of biweight mean
    % last eqn, p. 208

    varyh = n^.5*nom^.5 / ((den1*den2)^.5); % Dan: p.417 Kafadar
approach

    df = 0.7 * (nz -1); % degrees of freedom


   % if little change in mean, exit loop
    if abs (ymn - ymnold) < sens
        return
    end
end
```

```
% hugershoff.m
% This function fits a tree ring time series to the growth trend
equation
% developed by Warren (1980) TRR.

% Function written Nov 12, 2013.
% Function last revised Nov 12, 2013.

function qq = hugershoff(beta,x)

% Assign parameters from beta vector.
a=beta(1);
b=beta(2);
c=beta(3);
k=beta(4);
qq=a*((x).^b).*exp(-c*(x))+k;
% qq=a*((x+1).^b).*exp(-c*(x+1))+k;
%q=log(a)+b*log(x)%-c*x;
%qq=exp(
```

```
% nonlinear_exp.m
% This function fits a tree ring time series to the non-linear
% equation used by Ed Cook in his ARSTAN program.

% Function written Jan 12, 2004.
% Function last revised Jan 29, 2004.

function qq = nonlinear_exp(beta,x)

% Assign parameters from beta vector.
a=beta(1);
b=beta(2);
d=beta(3);
qq = a*exp(-b*x)+d;
```

```
% ringwidth_import_999.m
% This function imports decadal format tree ring data for manipulation
% as a matrix in Matlab.  The number of header lines must be specified
% as an input by the user.  The end of each series must be flagged
% with 999.  Measurements are stored as one hundreth of a
% millimeter.  The filename can either be specified as an input or
% found using a gui. The LAST LINE of the input text file must also
% be blank!

% Function written Mar 4, 2004.
% Function last revised May 24, 2012.

function [col_header,rings]=ringwidth_import_999(header,varagin)

if nargin==1
    [filename,path]=uigetfile('*.txt','Select ".txt" file');
elseif nargin==2
    filename=varagin;
else
    disp('Too many parameters entered (DLD).')
end

% Read in header lines
headers=textread(filename, '%q',10)';
% disp([headers]) % Display 1st 10 words as screen output.
[label yr y0 y1 y2 y3 y4 y5 y6 y7 y8 y9]=...
    textread(filename,...
    '%8s %4d %5d %5d %5d %5d %5d %5d %5d %5d %5d %5d',...
    'headerlines',header);
% Place decadal format widths into one matrix
widths=[y0 y1 y2 y3 y4 y5 y6 y7 y8 y9];

% Extract unique labels of each core.
importedrows=length(label);
a=1;b=1;
while(a<=importedrows)
    core(b)=label(a);
    corestr(:,b)=strcmp(label(a),label);
    a=max(find(corestr(:,b)==1))+1;
    b=b+1;
end

% Find range of years over all cores and set as col 1 in rings.
% As it is difficult to know how many years are in the last row
% of measurments for a core, assume that the last decade has 10
% measurements.
rings=(min(yr):(max(yr)+10))';

% Transfer widths into vectors by core
for i=1:length(core)
    core_rows=find(corestr(:,i));
    core_yr=yr(core_rows);
    core_widths=widths(core_rows,:);
    % Find # of measurements in a row and assign to vector series.
    k=1;series=0;
    for j=1:length(core_rows)
        % Look for end of series flag
        flag=find(core_widths(j,:)==999);
        if flag>0
            msmts=flag-1;
```

```
            elseif (ceil(core_yr(j)/10)*10)-core_yr(j)==0
                msmts=10;
            else
                msmts=(ceil(core_yr(j)/10)*10)-core_yr(j);
            end
            series(k:(k+msmts-1))=core_widths(j,(1:msmts));
            k=msmts+k;

        end
        % Determine start and end of series
        sos=find(rings(:,1)==min(core_yr));
        length(series)+sos-1;
        eos=length(series)+sos-1;
        % Assign series to output matrix and convert to 1/1000th of a mm
        rings(sos:eos,i+1)=(series./100)';


       % Remove 999 from end of series
     %   for j=1:length(rings(1,:))
     %       for k=1:length(rings(:,1))
     %            if rings(k,j)==-99.99
     %                 rings(k,j)=0;
     %            end
     %        end
     %   end


    end
    % Construct column headers
    col_header(2:(length(core)+1))=core;
    col_header(1)={'Year'};
```

```
% ringwidth_import_9999.m
% This function imports decadal format tree ring data for manipulation
% as a matrix in Matlab.  The number of header lines must be specified
% as an input by the user.  The end of each series must be flagged
% with -9999.  Measurements are stored as one thousandth of a
% millimeter.  The filename can either be specified as an input or
% found using a gui. The LAST LINE of the input text file must also
% be blank!

% Function written Mar 4, 2004.
% Function last revised May 24, 2012.

function [col_header,rings,flag]=ringwidth_import_9999(header,varagin)

if nargin==1
    [filename,path]=uigetfile('*.txt','Select ".txt" file');
elseif nargin==2
    filename=varagin;
else
    disp('Too many parameters entered (DLD).')
end

% Read in header lines
headers=textread(filename, '%q',10)';
% disp([headers]) % Display 1st 10 words as screen output.
[label yr y0 y1 y2 y3 y4 y5 y6 y7 y8 y9]=...
    textread(filename,...
    '%8s %4d %5d %5d %5d %5d %5d %5d %5d %5d %5d %5d',...
    'headerlines',header);
% Place decadal format widths into one matrix
widths=[y0 y1 y2 y3 y4 y5 y6 y7 y8 y9];

% Extract unique labels of each core.
importedrows=length(label);
a=1;b=1;
while(a<=importedrows)
    core(b)=label(a);
    corestr(:,b)=strcmp(label(a),label);
    a=max(find(corestr(:,b)==1))+1;
    b=b+1;
end

% Find range of years over all cores and set as col 1 in rings.
% As it is difficult to know how many years are in the last row
% of measurments for a core, assume that the last decade has 10
% measurements.
rings=(min(yr):(max(yr)+10))';

% Transfer widths into vectors by core
for i=1:length(core)
    core_rows=find(corestr(:,i));
    core_yr=yr(core_rows);
    core_widths=widths(core_rows,:);
    % Find # of measurements in a row and assign to vector series.
    k=1;series=0;
    for j=1:length(core_rows)
        % Look for end of series flag
        flag=find(core_widths(j,:)==-9999);
        if flag>0
            msmts=flag-1;
```

```
        elseif (ceil(core_yr(j)/10)*10)-core_yr(j)==0
            msmts=10;
        else
            msmts=(ceil(core_yr(j)/10)*10)-core_yr(j);
        end
        series(k:(k+msmts-1))=core_widths(j,(1:msmts));
        k=msmts+k;
    end
    % Determine start and end of series
    sos=find(rings(:,1)==min(core_yr));
    length(series)+sos-1;
    eos=length(series)+sos-1;
    % Assign series to output matrix and convert to 1/1000th of a mm
    rings(sos:eos,i+1)=(series./1000)';
end
% Construct column headers
col_header(2:(length(core)+1))=core;
col_header(1)={'Year'};
```

```
% v105pn.m
% This function extracts a single tree-ring time series from
% ringwidth_import.m and places it in a vector for time series
analysis.
% The 'filename' used to load tree-ring data for processing should
refer to
% the file containing data imported using the function
ringwidth_import.m.
% Following the approach used in ARSTAN (Ed Cook, Columbia
University),
% the function power transforms and removes the mean to create
transformed
% residuals.  The function then detrends with an iterative neg.
exponential
% fit, or if that does not fit or fails to find a solution, then a
linear
% regression with either a positive or negative slope is fit to the
data.
% Using the maximum entropy model solution otherwise known as the Burg
% method, the autoregressive model that is the best fit for the series
is
% determined.  Using the best fit model, the function searches for
% autoregressive outliers iteratively.  These outliers may either be
pulse
% events (1 yr) or CSTs (> minimum no. of yrs).  After the first pass,
% the outliers are removed and the series is reconstituted.  The best
ar
% order is then redetermined and the function searches for additional
% outliers.  The # of iterations is set by the user (8 should be
enough).
% This version uses a power transformation to minimize
% the heteroscedastic nature of my time series. 'fig' is a flag that
% specifies whether you want a figure (=1) or not (=0).  Missing years
are
% set to the average of neighboring rings.  The central limit theorem
% is used to search the residuals for trend outliers.  This version
also
% uses David Meko's (University of Arizona) biweight mean code and
% currently runs with a window of 9 to 30 yrs.  Estimated values for
% missing rinngs are removed in the output series.  This version uses
a
% modified Hugershoff curve with a potentially nonzero asymptote to
% detrend + and - disturbance events. It also returns the transformed
% standardized series.

% Function written Sep 10, 2002.
% Function last revised Jun 6, 2014.

function [YEARS,transformed,detrended,St,Str,Dtr,Atr,age,outs]=...
    v105pn(core,fig,iter)
global PARAM; PARAM=0; % vector of parameters for best order AR model.
global ORDER; ORDER=0; % best order of AR model determined by AIC.
global YEARS; YEARS=0; % calendar years of tree growth from datafile

% Load tree-ring data (returns vars *col_header* and *rings*)
load filename.mat %Insert filename here

% Find pointer to start and end of series
sos=find(rings(:,(core+1))>0, 1);
eos=find(rings(:,(core+1))>0, 1, 'last');

```

```
% Assign years and raw widths to respective vectors.
YEARS=rings(sos:eos,1);
raw=rings(sos:eos,core+1);

disp(['Core: ' char(col_header(core+1))])
nyrs=length(YEARS);
disp(['Total no. of measured years: ' int2str(nyrs)])
disp(['First year is ' num2str(YEARS(1))])
disp(['Last year is ' num2str(YEARS(nyrs))])

% Estimate missing ring widths using mean of neighboring rings
mss=NaN(length(raw),1);

if find(raw==0)
   m1=find(raw==0);
   disp(['Missing rings at years ' num2str([YEARS(m1)'])])
   for nm=1:length(m1)
       prior=mean(raw(find(raw(1:m1(nm)),1,'last')));
       subs=mean(raw(find(raw(m1(nm):length(raw)),1,'first')+m1(nm)-
1));
       mss(m1(nm))=mean([prior subs]);
   end
   raw=nansum([raw mss],2);
end

% Power transformation.
fdiff=0;
for x=1:(length(YEARS)-1) % Calculate 1st differences
    fdiff(x,1)=raw(x+1);
    fdiff(x,2)=abs(raw(x+1)-raw(x));
end

s=1;
for q=1:(length(YEARS)-1)
    if (fdiff(q,1)~=0) && (fdiff(q,2)~=0)
        nz_fdiff(s,:)=fdiff(q,1:2);% non-zero ring widths
        s=s+1;
    end
end
log_fdiff=[log(nz_fdiff(:,1)) log(nz_fdiff(:,2))];

X=[ones(length(log_fdiff(:,1)),1) log_fdiff(:,1)];
bb = regress(log_fdiff(:,2), X);
optimal_line = bb(2)*log_fdiff(:,1)+bb(1);

optimal_pwr = 1-bb(2);
disp(['Optimal Power = ' num2str(optimal_pwr)])
if optimal_pwr <= 0.05
    transformed=log10(raw);
    tzero=log10(0.001);
    disp('Series was log10 transformed')
elseif optimal_pwr>1
    optimal_pwr=1;
    transformed=(raw.^(optimal_pwr));
    tzero=0.001.^(optimal_pwr);
    disp('Series was power transformed with power =1')
else
    transformed=(raw.^(optimal_pwr));
    disp(['Series was power transformed with power = ' ...
        num2str(optimal_pwr)])
```

```
    tzero=0.001.^(optimal_pwr);
end
transm=mean(transformed);

% Nonlinear detrending option.
% Function nlinfit employs nonlinear least squares data fitting by the
% Gauss-Newton Method.
crashed=zeros(nyrs,1);
wlngth=zeros(nyrs,1);
trendtype=0; % Neg exp = 1, neg linear reg = 2, or pos linear reg = 3
minyr=30; % minimum # of yrs to fit to nlinfit
if minyr>nyrs
    disp('Insufficient # of years to fit minimum nonlinear age
trend.')
end
b=zeros(nyrs,3);
mse=NaN(nyrs,1);
warning off
for i=minyr:nyrs
    try
        lastwarn('')
        beta = [.5 .1 1];
        xyrs = 1:i; % set years from 1 to length of series
        [b(i,1:3),~,~,~,mse(i)]=nlinfit(...
            xyrs(1:i),transformed(1:i)','nonlinear_exp',beta);
        crashed(i)=1;
        msgstr = lastwarn;
        wlngth(i)=length(msgstr);
    catch % Stops code from crashing because of problems fitting exp
curve
        crashed(i)=2;
    end
end
warning on
i_c=0;

% Dissallow curve to be concave up and make sure nlinfit
% converges by making b(2) sufficiently large.
% constant b(3) must be >=0 in original mm
i_c=find(crashed==1 & b(:,1)>=0 & b(:,2)>0.001 & b(:,3)>=tzero &
wlngth==0);% & b(:,2)<0.5);
[mmse,imse]=min(mse(i_c));

if fig==1 % fig=1 if you want a figure as output
    figure('Position', [10 150 600 600])
    subplot(3,1,1)
    plot(YEARS,raw,'k','LineWidth',2)
    ylabel('\bf Ring width (mm)')
    fig1atext = {['Optimal power = ', num2str(optimal_pwr,4)]};
    text(range(YEARS)/3+YEARS(1), max(raw)/1.2,fig1atext)
end

if i_c(imse)>0
    disp(['Lowest error from fit = ' num2str(mmse)])
    disp(['Best age trend fit from years ' num2str(YEARS(1)) ' to '
...
        num2str(YEARS(i_c(imse)))])
    disp(['Best fit extends for ' num2str(i_c(imse)) ' years'])
    best=b(i_c(imse),:);

    trendtype=1;
```

```
    y_exp=nonlinear_exp(best,xyrs);
    detrended=transformed-y_exp';
    disp('Initial Age Detrending')
    disp(['Y = ', num2str(best(1),4), '*exp(-', num2str(best(2),4),...
                '*x)+', num2str(best(3),4)]);
    if fig==1 % fig=1 if you want a figure as output
        subplot(3,1,2)
        [h312a, h312h1, h312h2] = plotyy(YEARS,[transformed
y_exp'],YEARS(i_c),mse(i_c));
        set(h312h1(1),'LineWidth',2)
        set(h312h1(1),'Color',[0 0 0])
        set(h312h1(2),'Color',[.2 .2 1])

set(h312h2(1),'LineStyle','none','Marker','.','MarkerFaceColor',[1 .2
.2])
        fig1btext = {['Y = ', num2str(best(1),4), '*exp(-',
num2str(best(2),4),...
                '*x)+', num2str(best(3),4)]};
        text(range(YEARS)/3+YEARS(1), max(transformed)/1.2,fig1btext)
        line([YEARS(i_c(imse)) YEARS(i_c(imse))],...
            [y_exp(i_c(imse))+.2
y_exp(i_c(imse))+.2],'Color','k','Marker',...
            'v','MarkerEdgeColor',[1 .2 .2],'MarkerFaceColor',[1 .2
.2])
        set(get(h312a(1),'Ylabel'),'String','\bf Transformed width')
        set(get(h312a(2),'Ylabel'),'String','\bf Error Term Variance')
        subplot(3,1,3)
        plot(YEARS,detrended,'k','LineWidth',2)
        ylabel('\bf Transformed width')
        xlabel('\bf Year')
    end
else
    trendtype=2;
    xyrs=(1:nyrs)';
    % Linear detrending option used if neg. exponential curve
dissallwd.
    [b,~,~,~,stats] = regress(transformed,...
        [ones(length(YEARS),1) xyrs]);
    if b(2)>=0; trendtype=3; end % Find positive age trends
        y_lin=b(2)*xyrs +b(1);
        detrended=transformed-y_lin;
        disp('Initial Age Detrending')
        disp(['Y = ', num2str(b(2)), ' * X + ', num2str(b(1))]);
        if fig==1 % fig=1 if you want a figure as output
            subplot(3,1,2)
            h312b=plot(YEARS,transformed,'k',YEARS,y_lin,'k--');
            set(h312b(1),'LineWidth',2)
            fig1btext = {['Y = ', num2str(b(2)), ' * X + ',
num2str(b(1))]};
            text(range(YEARS)/3+YEARS(1),
max(transformed)/1.2,fig1btext)
            ylabel('\bf Transformed width')
            subplot(3,1,3)
            plot(YEARS,detrended,'k','LineWidth',2)
            ylabel('\bf Transformed width')
            xlabel('\bf Year')
        end
end
% Output age detrending info
age={char(col_header(core+1)); trendtype; YEARS(i_c(imse))};
```

```
% % Plot a histogram of the data to investigate its skew.
% figure('Position', [50 25 400 300]);
% hist(detrended)
% title('\bf Histogram of Detrended Ring Widths')

% Initialize arrays.
next_iter=1; %Switch to determine whether next iteration is needed
St=detrended; % St will be the iterated series (standardized)
Atr=NaN(length(raw),1); % Age trend re-expressed in raw units
rline=NaN(length(raw),1); % Just the slope of the intervention
tline=NaN(length(raw),iter); % Slope and constant of the intervention
outs=zeros(iter,5);

for q=1:iter % Iterate AR model 'iter' times to remove all outliers
    if next_iter==1
        bckcasted=0;ar_estimate=0;residuals=0;area_t=0;
        iter_i=St; % Initial values of series for ith iteration.
        disp(' ')
        disp(['Statistics for AR model iteration ' int2str(q) ':'])

        % Calculate best AR model order and return in the following
order:
        % residuals (white noise) and ar model estimates
        [ar_white, ar_model]=ar_order(St);

        % Use new coefficients to prewhiten ORIGINAL series without
        % downweighted originals.

        % Backcast for pth order years of AR model.
        % bckcasted=backcast(detrended);
        bckcasted=backcast(St);

        for g=ORDER:length(bckcasted) % g = observation year
            ar=0; % ar model estimate for order i, year g
            for k=1:ORDER % kth parameter of order ORDER
                if (g-ORDER)>0 % ensure obs yr > model order
                    ar=PARAM(k)*(bckcasted(g-k))+ar;
                end
            end
            if g-ORDER>0 % calculate model estimate and residuals
                if detrended(g-ORDER)==0 % Set missing rings to ar
estimate value
                    disp(['Missing ring at year: ' int2str(YEARS(g-
ORDER))])
                    bckcasted(g)=ar;
                end
                ar_estimate(g-ORDER)=ar;
                residuals(g-ORDER)=(bckcasted(g)-ar);
            end
        end
        ar_estimate=ar_estimate';
        residuals=residuals';
        if fig==1 % fig=1 if you want a figure as output
            figure('Position', [600 150 600 600])
            subplot(4,1,1)
            h411=plot(YEARS,St,'k',YEARS,ar_estimate,'k-.');
            set(h411(1),'LineWidth',2)
            title(['\bf' char(col_header(core+1)) ' iteration '
int2str(q)])
            ylabel('\bf Trans. width')
            xlabel('\bf Year')
```

```
            axis([min(YEARS) max(YEARS) min(St)*.9 max(St)*1.1])
        end

        % Find release outliers
        [downres, mres, otype]=outlier_clt(residuals,fig);
        f=find(downres~=0);
        if otype==1 && ~isempty(f) % Pulse Outlier Detected
            St(f)=ar_estimate(f);
        elseif otype>1 && length(f)>1 % Trend Outlier Detected
            w=[ones(length(f),1) (1:length(f))'];
            slope=regress(St(f),w);
            disp(['Constant and slope = ' num2str([slope(1)
slope(2)])])

            % Fit Hugershoff curve to remainder of series
            lngthw=min(f):length(St);
            lngthwf=(max(f)+1):length(St);
            lngthn=1:length(lngthw);
            lngthn=lngthn(:);
            opts = statset('nlinfit');
            opts.FunValCheck = 'off';
            opts.MaxIter = 400;
            bw=nlinfit(lngthn,St(lngthw),'hugershoff',[.1 .5 .1
.1],opts);
            disp(['Hugershoff Parameters: ' num2str(bw)])
            ar_est=ar_estimate(f(1));
            rline(lngthw)=-bw(1)*(lngthn.^bw(2)).*exp(-bw(3)*lngthn)-
bw(4);

            % If nlinfit returns NaN, then try again with diffent
initial parameters.
            if find(isnan(rline(lngthw)))>0; rline(lngthw)=0;
                disp('Default initial parameters for Hugershoff curve
failed')
                disp('Fitting alternate, robust initial parameters [.1
.5 .1 .1]')
                opts.RobustWgtFun = 'bisquare'
                bw=nlinfit(lngthn,St(lngthw),'hugershoff',[.1 .5 .1
.1],opts);
                disp(['Hugershoff Parameters: ' num2str(bw)])
                ar_est=ar_estimate(f(1));
                rline(lngthw)=-bw(1)*(lngthn.^bw(2)).*exp(-
bw(3)*lngthn)-bw(4);
            end

            % If nlinfit returns NaN, then end outlier iterations and
quit.
            if find(isnan(rline(lngthw)))>0; rline(lngthw)=0;
               disp('Unable to fit Hugershoff curve')
               ar_est=0;
               next_iter=0;
               outs(q,1:5)=[0 0 0 0 0];
            end

            if f(1)>1
                St(lngthw)=rline(lngthw)+St(lngthw)+ar_est;
                tline(lngthw,q)=-rline(lngthw);
            elseif f(1)==1 % If trend occurs in 1st yr of series
                St(lngthw)=rline(lngthw)+St(lngthw);
                tline(lngthw,q)=-rline(lngthw);
            end
```

```
            outs(q,1:5)=[YEARS(min(f)) YEARS(max(f)) slope(1) slope(2)
otype];
        end

        if isempty(f) % Determine whether any outliers...
            next_iter=0; % were detected on this iteration
        end

        if q==iter && ~isempty(f)
            disp('Need to run additional iterations to resolve
series!')
        end

        if fig==1 % fig=1 if you want a figure as output
            subplot(4,1,4)
            hold on
            if ~isempty(f) && min(f)>1 % Draw detrended regression
line
                line([YEARS(min(f)) YEARS(max(f))],[ar_est ar_est],...
                    'Color',[.6 .6 .6],'LineStyle','--','LineWidth',2)
            else % Draw same line, but set to first year of series
                line([YEARS(1) YEARS(max(f))],[0 0],...
                    'Color',[.6 .6 .6],'LineStyle','--','LineWidth',2)
            end

h414=plot(YEARS,iter_i,'k',YEARS,St,'k',YEARS,tline(:,q),'k');
            set(h414(1),'LineWidth',2)
            set(h414(3),'LineWidth',2,'Color',[.6 .6 .6])
            ylabel('\bf Trans. width')
            xlabel('\bf Year')
            ymin=min([min(iter_i) min(St)])*.9;
            ymax=max([max(iter_i) max(St)])*1.1;
            axis([min(YEARS) max(YEARS) ymin ymax])
            box on
            hold off

            subplot(4,1,2)
            h412=plot(YEARS,residuals,'k-
.',YEARS,zeros(1,length(YEARS)),'k',...
                YEARS,mres);
            set(h412(3),'Color',[.6 .6 .6])
            set(h412(3),'LineWidth',2)
            axis([min(YEARS) max(YEARS) min(residuals)*1.1
max(residuals)*1.1])
            ylabel('\bf Residuals')
            xlabel('\bf Year')
        end
    end
end


if fig==1 % fig=1 if you want a figure as output
    % Shows final iterated series in transformed units
    figure('Position', [1200 150 600 400])
    subplot(2,1,1)
    transDt=detrended-St; % transformed outlier series
    hpentult=plot(YEARS,detrended,'k',YEARS,St,'k--');
    set(hpentult(1),'LineWidth',2)
    set(hpentult(2),'LineWidth',2)
```

```
    legend('Age-detrended series','Standardized series',...
        'Location','NorthWest')
    legend('boxoff')
    ylabel('\bf Transformed width')
end

% Shows final iterated series in original units (mm presumably)

if trendtype==1 % negative exponential trend
    Stt=y_exp'+St; % Size trend & first detrending
    if optimal_pwr <= 0.05
        Str=10.^(Stt);% Size trend in original (raw) units
        Atr=10.^(y_exp');% Age trend in original (raw) units
    else
        Stt(Stt<=0)=0; % Set neg values to zero
        Str=(Stt).^(1/optimal_pwr);
        Atr=(y_exp').^(1/optimal_pwr);
    end
elseif trendtype==2 || trendtype==3 % linear regression trend
    Stt=y_lin+St; % Size trend & first detrending
    if optimal_pwr <= 0.05
        Str=10.^(Stt);% Size trend in original (raw) units
        Atr=10.^(y_lin);% Age trend in original (raw) units
    else
        Stt(Stt<=0)=0; % Set neg values to zero
        Str=(Stt).^(1/optimal_pwr);
        Atr=(y_lin).^(1/optimal_pwr);
    end
else
    disp('Error in trend type designation')
end

raw(mss>0)=NaN; % Remove estimated values of missing rings
Str(mss>0)=NaN; % Remove estimated values of missing rings
Dtr=raw-Str; % Remove estimated values of missing rings

if fig==1 % fig=1 if you want a figure as output
    subplot(2,1,2)
    h_end=plot(YEARS,Dtr,YEARS,Str,'k--
',YEARS,raw,'k');%,YEARS,Atr,'b');
    set(h_end(1),'Color',[.6 .6 .6])
    set(h_end(1),'LineWidth',2)
    set(h_end(2),'LineWidth',2)
    set(h_end(3),'LineWidth',2)
    legend('Disturbance index','Standardized series','Original
series',...
        'Location','NorthWest')
    legend('boxoff')
    ylabel('\bf Ring width (mm)')
    xlabel('\bf Year')
end

% ar_order.m
%%%%%%%%%%%%%%%%%%%%%%%%%%%%%%%%%%%%%%%%%%%%%%%%%%%%%%%%%%%%%
% This subfunction is based on series_ar.m and determines the
% autoregressive parameters for the best model order as calculated
using
% AIC criteria. The function returns the residuals, and AR model
% estimate of the best order found with AIC criteria.
function [out_res, out_est]=ar_order(series)
global PARAM
```

```
global ORDER
global YEARS

% Initializes variables for autoregressive modeling.
ar_param=0; residuals=0;

% Calculate Autoregressive parameters for orders 1 through 10.
for ar_order=1:10
    ar_param(ar_order,1:ar_order+1)=-arburg(series,ar_order);
end

%Remove first column of minus ones from ar_param.
ar_param(:,1)=[];

% Calculate residuals for particular AR order model.
for i=1:10 % i = ar model order
    for g=1:length(YEARS) % g = observation year
        ar=0; % ar model estimate for order i, year g
        for k=1:length(ar_param(1,:)) % kth parameter of order i
            if (g-k)>0 % ensure obs yr > model order
                ar=ar_param(i,k)*(series(g-k))+ar;
            end
        end
        if g-i>0 % calculate residuals
            residuals(g,i)=(series(g)-ar);
            ar_estimate(g,i)=ar;
        end
    end
    % Calculate the total variance of the residuals by model order
    resid_var(i)=var(residuals(:,i));
end

% Calculate variance of the residuals of a particular AR order model.
% Reference Box & Jenkins & Reinsel 1994 pp. 200-201.
% Using Akaike Information Criteria
% Equation now uses natural log and simply 'n' in the denominator.
% t+1 (or # of params+1) is a penalty factor for estimating the mean.
aic=0;
for t=1:length(resid_var)
    aic(t)=log(resid_var(t))+(2*(t+1))/length(YEARS);
end
% Find the first minimum AIC order (ie first saw-tooth-shaped dip).
% If AIC values monotonically decrease, set best_order=9.
best_order=0;
for s=2:length(aic)
    if((aic(s)>=aic(s-1)) && (best_order==0))
        best_order=s-1;
    end
end

if best_order==0;
    best_order=9;
end

ORDER=best_order;
PARAM=ar_param(best_order,1:best_order);

disp(['AR Model Parameters: ' num2str(PARAM)])

out_res=residuals(:,best_order);
```

```
out_est=ar_estimate(:,best_order);

% outlier_clt.m %%%%%%%%%%%%%%%%%%%%%%%%%%%%%%%%%%%%%%%%%%%%%%%%%%%%%%
%
% This subfunction determines the auto regressive outliers in the
% residuals that are greater than a given number of std devs using the
% central limit theorem.
% 99% of the observations lie within 2.58(std_res)
% 97.5% of the observations lie within 2.24(std_res)

function [dres, rmr, type]=outlier_clt(in,fig2)
global YEARS

% initialize variables
type=0; % Type of outlier detected (1=pulse, 2=trend)
lngth=length(YEARS);
a=9; b=30;
% a=9; b=30; %b=lngth/3; %b=lngth-40; % min and max of trend window
if b>lngth/4
    b=floor(lngth/4);
    disp(['Maximum outlier detection length reduced to ' num2str(b) '
due to low ring #'])
end
lt=a; % Length of trend
window=0;
nse=3.29;
% nse=1.96; % 95 pct CI
% nse=2.58; % 99 pct CI8
% nse=3.29; % 99.9 pct CI
dres=zeros(lngth,1); % downweighted residuals
mr=zeros(lngth,1); % residuals mean in window
rmr=zeros(lngth,1);
rmu=0;
rshat=0;

% initialize masked to ones.
marker=zeros(length(YEARS),1);
masked=zeros(length(YEARS),1);

std_res = (var(in))^0.5; % Calculate std dev of residuals

% for u=1:length(YEARS) % Detect pulse outliers
%     rres=in(u)/(nse*std_res); % calculates relative residuals
%     if  rres>=1.0
%         dres(u)=1;
%         type=1;
%         disp(['Positive Pulse in ' int2str(YEARS(u))])
%         disp(['Outlier value = ' num2str(rres)])
%     elseif rres<=-1.0
%         dres(u)=1;
%         type=1;
%         disp(['Negative Pulse in ' int2str(YEARS(u))])
%         disp(['Outlier value = ' num2str(rres)])
%         % elseif abs(rres)<1.0
%         % psi=rres;
%         % The code below simply produces psi = rres.  Why did Ed
code it
%         % this way in his robar function?
%         % psi=rres*exp(-exp(3.0*(abs(rres)-3.0)));
%     else
%         disp('No pulse outliers detected')
```

```
%      end
% end

if a<=b
    for v=a:b
        z=v-a+1;
        for u=1:(lngth-v)%+1) % Changed 4-13-13
            window=in(u:(u+v-1));
            mr(u,z)=mean(window);
        end
        % [muhat(z),sigmahat(z)] = normfit(mr(:,z)) % Arithmetic mean
        % Uses Tukey's bi-weight mean instead (Hoaglin 1983, Meko's
code)
        [ymn(z),varyh(z),~,~,~,se]=bisqmean_CID(mr(:,z));
        [mam(z),imax(z)]=max(mr(:,z)); % Find max. means & their
locations
        [mim(z),imin(z)]=min(mr(:,z)); % Find min. means & their
locations
    end

    poso=(mam-ymn)./varyh; % Determines # deviations from mean of
means
    nego=(ymn-mim)./varyh;
    [relmam, rimax]=max(poso); % Find max. of positive dev.s & their
locations
    [relmim rimin]=max(nego); % Find max of negative dev.s & their
locations
    disp(['Max departure = ' num2str(relmam)])
    disp(['Min departure = ' num2str(relmim)])
    if (poso(rimax)>=nse)  % && (relmam>=relmim) % Comment && for only
+ outliers
        type=2;
        lt=rimax+a-1; % length of trend
        dres(imax(rimax):(imax(rimax)+lt-1))=ymn(rimax);
        disp(['Release detected in ' int2str(YEARS(imax(rimax)))...
            ' for ' int2str(lt) ' years'])
        rmu=ymn(rimax);
        rshat=varyh(rimax);
        rmr=mr(:,rimax);
        % disp(['rmu= ' num2str(rmu)])
        % disp(['rshat= ' num2str(rshat)])
%     elseif (nego(rimin)>=nse) % Comment elseif for only + outliers
%         type=3;
%         lt=rimin+a-1;
%         dres(imin(rimin):(imin(rimin)+lt-1))=ymn(rimin);
%         disp(['Suppression detected in '
int2str(YEARS(imin(rimin)))...
%             ' for ' int2str(lt) ' years'])
%         rmu=ymn(rimin);
%         rshat=varyh(rimin);
%         rmr=mr(:,rimin);
%         disp(['rmu= ' num2str(rmu)])
%         disp(['rshat= ' num2str(rshat)])
    else
        rmu=ymn(1);
        rshat=varyh(1);
        rmr=mr(:,1);
        disp(['No trend outliers detected up to ' int2str(b) ' yrs'])
    end

end
```

```
if fig2==1 % fig=1 if you want a figure as output
    subplot(4,1,3)
    hold on
    hist(rmr)
    h413 = findobj(gca,'Type','patch');
    set(h413,'FaceColor','k')
    box on
    % title('\bf Histogram of Running AR Residual Means')
    line([rmu-nse*rshat rmu+nse*rshat],[10 10],'Color',[.6 .6 .6])
    plot(rmu,10,'o','Color',[.6 .6 .6])
    ylabel('\bf Frequency')
    xlabel(['\bf' int2str(lt) '\bf Yr Residual Means'])
    hold off
end

% backcast.m
%%%%%%%%%%%%%%%%%%%%%%%%%%%%%%%%%%%%%%%%%%%%%%%%%%%%%%%%%%%%
% This subfunction estimates the first elements of a series for which
the
% residuals could not be calculated owing to the use of ar modeling.
function bckcasted=backcast(seriesb)
global PARAM
global ORDER
global YEARS

% Invert time series for backcasting.
flipped=flipud(seriesb);

% Add in backcasted AR estimates as new values at end of inverted
series.
for g=(length(YEARS)+1):(length(YEARS)+ORDER) % g = backcasted years
    ar=0; % ar model estimate for order i, year g
    for k=1:ORDER % kth parameter of order ORDER
        ar=PARAM(k)*(flipped(g-k))+ar;
    end
    flipped(g)=ar;
end

% Re-invert series and return as output.
bckcasted=flipud(flipped);
% disp('Backcasted Values:')
% for h=ORDER:-1:1
%     disp(['Year -' int2str(h) ': ' num2str(bckcasted(h))])
% end
```

```
% v105pn_chron.m
% This function can be used to process multiple series (whereas
v105pn.m is
% used to process single series).
% The function calculates each autoregressive outlier for each
% core in a dataset and lumps those results by tree.  This version
also
% returns the transformed standardized series for each core in St.
% The ‘filename’ used in this function and in function v105pn.m to
load
% the data file must match and should contain data imported using
function
% ringwidth_import.m.

% Function written Mar 10, 2004.
% Function last revised Jun 10, 2014.

function
[yrs,tres,det,St,Straw,Dtraw,sigDtraw,Atraw,out,dbh_rel,age_rel]...
    =v105pn_chron

% Load tree-ring data (returns vars *col_header* and *rings*)
load filename.mat %Insert filename here

iter=8; % maximum number of iterations per series.
years=rings(:,1); % years for entire chronology
rings(:,1)=[]; % remove year column
col_header(1)=[]; % remove year label from array
ncores=size(rings,2); % # cores in group
nyrs=size(rings,1); % total # of years in chronology
expval=NaN(1,ncores); % value of last year that neg exp curve fits
yrs=NaN(nyrs,ncores); % years for each cores
dbh_rel=NaN(nyrs,ncores); % dbh at release for each core
age_rel=NaN(nyrs,ncores); % age at release for each core
tres=NaN(nyrs,ncores); % Transformed residuals for each core
det=NaN(nyrs,ncores); % Detrended series for each core
St=NaN(nyrs,ncores); % Undisturbed series for each core in transformed
units
Straw=NaN(nyrs,ncores); % Undisturbed series for each core
Atraw=NaN(nyrs,ncores); % Age series for each core
Dtraw=NaN(nyrs,ncores); % Disturbance series for each core
% agestats=NaN(2,ncores); % power and trend type for transformed core
agestats=cell(3,ncores); % power and trend type for transformed core
% agestats(3,:)={'0000'};
out=NaN(iter,7,ncores); % Outlier statistics

for i=1:ncores
    disp(' ')
    disp(['Series #' num2str(i) '--------------------------------------
--'])
    % Find pointer to start and end of series
    s=find(rings(:,i)>0,1);
    e=find(rings(:,i)>0,1,'last');

[yrs(s:e,i),tres(s:e,i),det(s:e,i),St(s:e,i),Straw(s:e,i),Dtraw(s:e,i)
,...

Atraw(s:e,i),agestats(:,i),out(1:iter,1:5,i)]=v105pn(i,0,iter);

    b=find(out(:,5,i)==2);% find all releases for a core
    if b>0
```

```
            for c=1:length(b) % iterate through each release
                startyr=find(years==out(b(c),1,i));
                dbh_rel(startyr,i)=sum(rings(s:startyr,i))/1000;
                age_rel(startyr,i)=length(rings(s:startyr,i));
            end
        end
        clear b
        clear startyr
    end

    figure('Position', [10 5 700 800])
    subplot(2,1,1)
    nanrings=cumsum(rings,1); % cumulative dbh
    coreage=rings;
    coreage(find(coreage>0))=1;
    coreage=cumsum(coreage,1); % count age of each core
    coreage(coreage==0)=NaN;
    av_ca=nanmean(coreage,2);
    v_ca=nanstd(coreage,1,2);
    nanrings(nanrings==0)=NaN;
    av_dbh=nanmean(nanrings,2)/1000;
    v_dbh=nanstd(nanrings,1,2)/1000;
    hold on
    fill([years; flipud(years)],[v_dbh+av_dbh; flipud(av_dbh-v_dbh)],...
    [.7 .7 .7],'EdgeColor','none')
    plot(years,av_dbh,'k',years,dbh_rel,'k--o')
    ylabel('\bf Av. Inside Diameter (m)')
    xlabel('\bf Year')
    hold off

    subplot(2,1,2)
    hold on
    fill([years; flipud(years)],[v_ca+av_ca; flipud(av_ca-v_ca)],...
    [.7 .7 .7],'EdgeColor','none')
    plot(years,av_ca,'k',years,age_rel,'k--o')
    ylabel('\bf Av. Age')
    xlabel('\bf Year')

    rel=[0 0 0 0];
    sup=[0 0 0 0];
    d=1; % release counter
    f=1; % suppression counter

    % Summarize outlier descriptive statistics
    for a=1:size(Dtraw,2)% # of cores
        b=find(out(:,5,a)==2);% find all releases for a core
        if b>0
            for c=1:length(b) % iterate through each release
                startyr=out(b(c),1,a);
                endyr=out(b(c),2,a);
                Dt_diff=out(b(c),6,a)-out(b(c),7,a);
                gc=(Dt_diff)/out(b(c),7,a);
                rel(d,1:4)=[a startyr endyr gc];
                d=d+1;
            end
        end
        clear b

        g=find(out(:,5,a)==3);
        if g>0
            for h=1:length(g)
```

```
                startyr2=out(g(h),1,a);
                endyr2=out(g(h),1,a);
                Dt_diff2=out(g(h),6,a)-out(g(h),7,a);
                gc2=(Dt_diff2)/out(g(h),7,a);
                % Dt_inc=Dt_diff*(endyr2-startyr2+1);
                sup(f,1:4)=[a startyr2 endyr2 gc2];
                f=f+1;
            end
        end
        clear g
    end
    rings(find(~rings))=NaN; % Convert rings matrix zeros to NaNs

    % Find and average all cores with pos or neg outliers
    subset=unique([rel(:,1); sup(:,1)]);
    subset=subset(find(subset));% Find & remove nonzeros if no pos or neg outliers found
    if subset % Only graph if interventions found.
        sigDtraw=Dtraw(:,subset);
        sigDtm=nanmean(Dtraw(:,subset),2);

        depth=size(Dtraw,2)-sum(isnan(Dtraw),2); % Total sample depth
        % samples with outliers
        subdepth=size(Dtraw(:,subset),2)-sum(isnan(Dtraw(:,subset)),2);

        figure('Position', [10 5 700 800])
        subplot(4,1,1)
        h_end=plot(years,nanmean(rings-Atraw,2),'k',years,nanmean(Straw-Atraw,2),'k--');
        set(h_end(1),'LineWidth',2)
        set(h_end(2),'LineWidth',2)
        legend('Mean Ct + Dt','Mean Ct','Location','NorthWest')
        legend('boxoff')
        ylabel('\bf Residuals (mm)')
        xlabel('\bf Year')

        subplot(4,1,2)
        [AX,H1,H2] = plotyy(years,sigDtm,years,depth);
        set(H1,'LineWidth',2)
        set(H1,'Color','k')
        set(H2,'Color','k')
        set(AX(1),'ycolor','k')
        set(AX(2),'ycolor','k')
        set(get(AX(1),'Ylabel'),'String',{'\bf Mean Dt', '(mm)'})
        set(get(AX(2),'Ylabel'),'String','\bf Sample Size')
        set(AX(2),'ylim',[0 ceil((ncores+1)/10)*10])
        set(AX(1),'XTickLabel',[])
        bounds=xlim;
        box off

        subplot(4,1,3)
        mindecade=bounds(1);
        maxdecade=bounds(2);
        edges=[mindecade:10:maxdecade]; % Bin outliers by decade
        pCCT=histc(rel(:,2),edges);
        nCCT=histc(sup(:,2),edges);

        hold on
        bar(edges+5,pCCT,'k')
        bar(edges+5,-nCCT,'k')
        xlim([bounds(1) bounds(2)])
```

```
    hold off
    ylabel('\bf +Dt Initiation Yrs')

    subplot(4,1,4) % show cores that are open grown initially
    agenum=cell2mat(agestats(2,:));
        edges=mindecade:10:maxdecade; % Bin outliers by year
    for i=1:size(yrs,2);
firstyr(i)=yrs(find(rings(:,i)>0,1,'first'),i);end
    opngrwn=firstyr(agenum==1);
    disp('Trees that likely established in open conditions')
    disp(col_header(agenum==1));
    clsdcan=firstyr(agenum==2|agenum==3);
    % Establishment dates binned by decade
    o=histc(opngrwn,edges); o=o(:);% open oaks
    u=histc(clsdcan,edges); u=u(:);% understory oaks
    Y=[u o];
    bar(edges+5,Y, 'stacked')
    axis([mindecade maxdecade 0 max(o+u+5)])
    ylabel('\bf Tree Recruitment')
    xlabel('\bf Year')
    ColorOrder2=...
        [0 0 0; 1 1 1];
    colormap(ColorOrder2)

else
    sigDtraw=0;
    sigDtm=0;
end
```